Review

Fluid Net Models: From Behavioral Properties to Structural Objects

Manuel Navarro-Gutiérrez [1],*, Antonio Ramírez-Treviño [2] and Manuel Silva [3]

[1] Escuela de Ingeniería y Ciencias, Tecnológico de Monterrey, Av. General Ramón Corona 2514, Zapopan 45201, Mexico

[2] Centro de Investigación y de Estudios Avanzados del Instituto Politécnico Nacional, Unidad Guadalajara, Av. del Bosque 1145, Zapopan 45019, Mexico; antonio.ramirezt@cinvestav.mx

[3] Instituto de Investigación en Ingeniería de Aragón (I3A), Universidad de Zaragoza, María de Luna 1, 50018 Zaragoza, Spain; silva@unizar.es

* Correspondence: manuel.navarro.gtz@tec.mx

Abstract: Increasing the production in manufacturing systems is one of the main demands in modern systems. The naive approach that this goal can be achieved when more or faster resources are used is not always valid. In fact, the complex interactions among system's elements may lead to paradoxical behaviors; for example, using faster machines could reduce the equilibrium throughput (number of part fabricated per unit time in steady state) of the system, or even worse, block all system activities, reducing it to zero. This work leverages the concepts about fluidization and analysis techniques used in Timed Continuous Petri nets (TCPN) presented in earlier works to study the behavior of the equilibrium throughput when more/faster machines are used. Herein, we illustrate how discontinuities induced bifurcations of the equilibrium throughput are due to the existence of paths that can increase/decrease the marking of certain subnets. In particular, if paths gaining/losing tokens are fired without a particular balance, then the equilibrium throughput exhibits discontinuities since the equilibrium marking loses hyperbolicity. Moreover, these discontinuities imply other undesired throughput behaviors; for example, the existence of non-monotonicities of the equilibrium throughput (when more/faster resources are used in the system, its equilibrium throughput is reduced). The discontinuities together with a homothecy property are used to explain non-monotonicities in the equilibrium throughput. A relevant aspect is that these undesired system behaviors appear when the net has structural objects named problematic configurations that are associated with certain subnets in which there are no P-semiflows. Although the number of these configurations increase exponentially in the size of the net, some reduction rules are introduced to remove configurations, while the problematic ones are kept (or can be recovered) in the reduced net. This saves computation time in the analysis and, more importantly, provides useful insights about the root of undesired behaviors. This work focus on systems that can be modeled with fluid (or continuous) mono T-semiflow Timed Continuous Petri nets. Even if under certain constraints, they are capable of capturing many characteristics of modern systems, such as interleaving of cooperation and competition.

Keywords: fluid models; Petri nets; structural properties

1. Introduction and Motivation

The more basic analysis of Discrete Event Systems (DES) focuses on properties such as *liveness*, *boundedness*, and, when timed, system *performance*. Considering Flexible Manufacturing Systems (FMSs), as an example, the performance may deal with the number of goods fabricated per unit time (i.e., the throughput) or the number of items in a storage (i.e., its marking). If the throughput should be increased, then it may be an initial idea to increase the speed of the machines or the number of resources. Unfortunately, it may not only decrease the system throughput, but even worse, reduce it to zero (deadlock).

An overview of these paradoxical throughput behaviors are studied in this work when the systems are modeled with Timed Continuous Petri nets (TCPN).

Petri nets (PN) are a fine and well-known formalism to model *Discrete Event Systems*, since they have a sound mathematical background, capturing in a compact manner basic system characteristics, such as causal relationships, synchronization, and concurrence. Moreover, their nice graphical representation provides a communication framework between engineers and practitioners. This work assumes that the reader is familiar with some basic concepts of PN, such as (structural) liveness, (structural) boundness, or reachability graph [1,2]. Unfortunately, as any other expressive DES formalism, they suffer from the so-called *state explosion* problem, particularly when they are heavily populated (heavily marked in PN terms). This problem is overcome with a classical relaxation: the *fluidization* of the system, i.e., both, the marking and the firing vectors are now considered non-negative real numbers. This leads to the concept of *Fluid* or *Continuous* PNs (CPNs). CPNs make some computational problems *decidable* or much tractable in practice [3].

When a quantitative notion of time is introduced in the paradigm of the CPN, then the evaluation of the system performance indices is also possible (throughput, response time, average marking), leading to the notion of *Timed* CPN (TCPN). We use the *infinite server semantics* (ISS), also known as *variable speed*, to express the firing rate of transitions. Under this consideration, the fluid systems are continuous piecewise linear with polyhedral regions. For certain net subclasses, which can model several types of manufacturing systems, ISS provides better approximations of the system throughput [4]. Nonetheless, depending on the system, other timing interpretations may be more adequate, for example, *finite server semantics* (FSS) in some hydraulic systems (see [5]) or *product semantics* (PS) in biologic systems (see [6]). In some sense, this work complements the overview [7] (for a more technical and detailed presentation, see [6]).

Performance evaluation is a major concern when analyzing DES. For instance, a study of the performance of manufacturing systems can be found in [8], where *generalized stochastic Petri nets* are used to model the systems. The analysis is based mainly on the simulation of the model to obtain the performance indices. Under the assumption of modeling with TCPN-ISS, ref. [9] presents the performance evaluation of manufacturing systems, where an insight of the relation between the structure of the model and the performance indices is discussed. That relation with the structure represents how the resources and the processes interact. The present work makes an effort to clarify how the performance of a system is affected when the resources or the velocity of processes are modified, relating them with the structure of the system.

This work focuses on the class of *Mono-T-Semiflow-Reducible* MTSR nets [10], since they allow to model a certain degree of *cooperative* and *competitive* relationships that arise in many practical systems, for instance flowshop or mass production systems. For the sake of simplicity, the results in this work are formulated for Mono-T-Semiflow nets; however, they can be easily extended to MTSR nets using the reduction rule already discussed in [10].

For the class of MTSR nets, the number of firings of transitions per time unit can be interpreted as the finished jobs per time unit in the flowshop, which can be used to measure the performance of the manufacturing system and is related to the equilibrium throughput of the TCPN system. In particular, qualitative properties of the equilibrium throughput such as *monotonicity*, *continuity*, and *deadlock-freeness*, as functions of the initial marking, firing transitions rates, and net structure, are herein systematically analyzed. The equilibrium throughput is:

- Monotonic, when increasing the initial marking and/or the transition firing rates leads to a non-slower system (a desired behavior); that is, more or faster resources in the system should at least not reduce the number of finished jobs per time unit;
- Continuous, when no abrupt changes of the equilibrium throughput are possible in the system when firing rates and/or the initial marking vary (again a desired system property);

- Deadlock-free, when no blocking situation can occur in the system (this property can be reinterpreted as "persistence" in chemical reaction networks [11]).

As a motivation, here, a cell composed of one input and one output stores of six slots each, one conveyor belt, a computer numerical control (CNC) machine, and a robot is presented. The cell is devoted to the manufacture of gears. The raw material resides in the input store. The robot retrieves the raw material from the input store and places it onto the conveyor. The conveyor is a two-site belt, and it leads the raw material into the CNC machine, which fabricates gears. The robot unloads the machine when it finishes a gear, and places the finished gear into the output store. Figure 1a shows a photo of this manufacturing cell.

A TCPN model of the manufacturing cell is presented in Figure 1b, and the description of places and transitions are presented in Tables 1 and 2, respectively. The firing of t_1 indicates that a part arrives to the cell and it is stored in the input store. The firing of t_2, t_3 and t_4 represent that a part is retrieved by the robot form the input store, deposited on the conveyor, and loaded into the CNC machine, respectively. The unloading of the CNC machine and the storing of a part in the output store are represented by the firing of t_5 and t_6, respectively. Finally, t_7 indicates that a part leaves the cell.

Table 1. Places and their description in the *TCPN* model of Figure 1b.

Place	Description
	Robot
p_8	Robot is idle
p_3	Robot retrieved a part from input store
p_6	Robot unloaded a part from CNC machine
	CNC machine
p_{11}	CNC is idle
p_5	CNC is processing a part
	Input Store
p_9	Free slots of the Input Store
p_2	Stored parts in Input Store
	Output Store
p_{12}	Free slots of the Output Store
p_7	Stored parts in Output Store
	Conveyor
p_{10}	Free sites in the conveyor
p_4	Occupied sites on the conveyor
	System capacity
p_1	Number of jobs that can be processed in the system

Table 2. Transitions and their description in the *TCPN* model of Figure 1b.

Transition	Description
t_1	A part arrives to the cell and it is stored into the input store
t_2	The robot retrieves a part from the input store
t_3	The robot deposits a part onto the conveyor
t_4	A part leaves the conveyor and is loaded into the CNC machine
t_5	The robot unloads a finished part from the CNC machine
t_6	The robot stores a part into the output store
t_7	A part is retrieved from the output store and leaves the cell

The net in Figure 1b is *structurally bounded*, i.e., for every initial marking, any reachable marking maintains a limited number of tokens in every place. In this model, tokens in place p_1 represent the raw material, the firing of transition t_2 represents the robot retrieving a part from the input store, and the firing of transition t_5 represents that the robot unloads the machine.
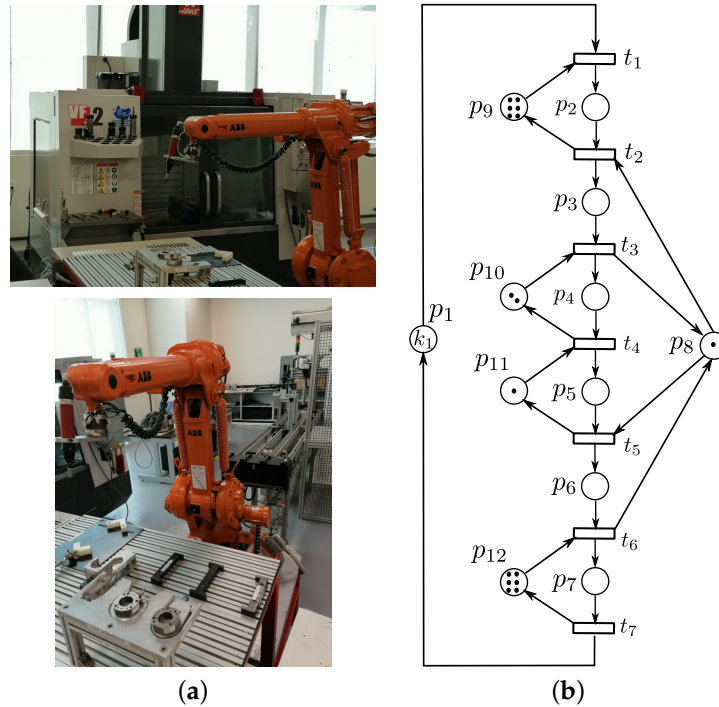

Figure 1. A manufacturing cell and its Petri net model. (**a**) Manufacturing cell. (**b**) Manufacturing cell model.

With regard to the *initial marking variation* and how the qualitative properties of the continuous equilibrium throughput varies, the considered initial marking is $m_0 = [k_1\ 0\ 0\ 0\ 0\ 0\ 1\ 6\ 2\ 1\ 6]^T$ and the firing rate is fixed to $\lambda = [1\ 2\ 1\ 1\ 1\ 1\ 1]^T$. In this case, $m_0(p_1) = k_1$ varies in the range $[0, 7]$, leading to a variation in the equilibrium throughput, which is depicted in Figure 2a. It shows that the equilibrium throughput is non-monotonic, even non-continuous with respect to the marking variations. Figure 2a is obtained by simulating the evolution of the piecewise linear system for several values of k_1 from zero to seven. The value of the equilibrium throughput is plotted for every value of k_1.
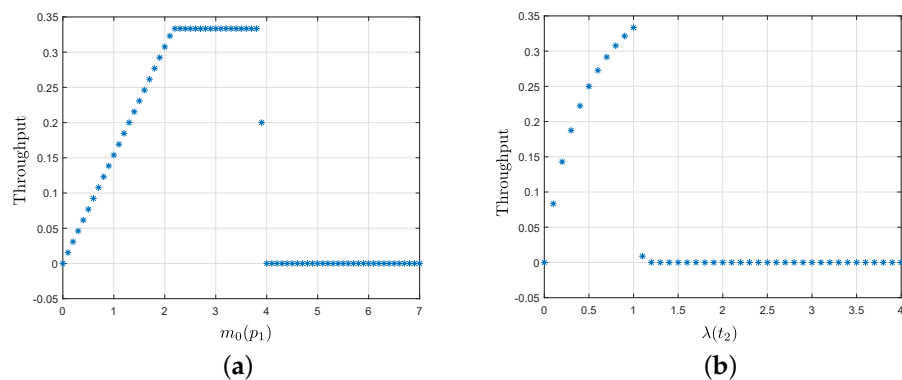

Figure 2. Equilibrium throughput of the Petri net model with respect to the initial marking and with respect to the firing rates. (**a**) Initial marking variation k_1. (**b**) Firing rate variation λ_2.

With regard to the *firing rates variation* and how the qualitative properties of the equilibrium throughput varies, the initial marking is fixed to $m_0 = [10\,0\,0\,0\,0\,0\,0\,1\,6\,2\,1\,6]^T$ and the firing rate is $\lambda = [1\,\lambda_2\,1\,1\,1\,1]^T$. In this case, $\lambda(t_2) = \lambda_2$ varies in the range $[0,\,4]$, leading to a variation in the equilibrium throughput, which is depicted in Figure 2b. This second figure shows that the equilibrium throughput is non-monotonic, even non-continuous with respect to the firing rate variations (there exists an abrupt change around $\lambda_2 = 1$). Figure 2b is obtained by simulating the evolution of the piecewise linear system for several values of λ_2 from zero to four. The value of the equilibrium throughput is plotted for every value of λ_2.

It is worth to notice that these non-monotonic, non-continuous behaviors are undesirable. In both cases, increasing the number of resources or their speeds, the throughput of the unforced system (i.e., non-controlled) is reduced to zero, that is, the manufacturing system reaches a blocking situation. Moreover, these behavioral properties of TCPN systems are closely related to behavioral properties of discrete systems, even when the net is structurally live (i.e., there exists initial markings that make the system live).

This example shows that the problem of non-monotonicity is originated when there are several tokens in $m_0(p_1)$ (increasing the system raw material) or $\lambda(t_2)$ is increased (there is a faster resource), allowing that t_2 fires more often than t_5. This reduces to zero the tokens in p_8, p_{10}, and p_{11}; hence, t_3 cannot be fired again and the TCPN is blocked.

Partially with a mix among a survey and tutorial style, this paper reviews in an integrated way efficient analysis techniques of some non frequently considered time-based qualitative properties of TCPN systems under infinite server semantics, among others, non-monotonicities and discontinuities on the equilibrium throughput (or marking). Focusing on the search of the net structural objects leading to such pathological/paradoxical behaviors, in essence, the results are based on [4,10,12–16]. The idea is searching for computational efficiency, while at the same time looking for a better understanding of the potential connections among structure and behaviors (the latter also depend on the initial marking). In order to approximate the sub-field to the practice, the present work is complemented with some new algorithms. For instance, Algorithms 1 and 2 allow to verify if a system is consistent and has not empty siphons at the initial marking; these are two required conditions of practical systems. Algorithm 3 allows to classify the structural objects (*configurations*) that determine the possible behaviors of the system. Algorithm 4 decides if a configuration can be *activated* to know the behaviors of the system.

This work deals with these undesired behaviors and their relation to the Petri net structure. Section 2 essentially provides the basic notation used. In Section 3, a discussion about the jumps in the equilibrium throughput is addressed. Discontinuity-induced bifurcations, earlier approached in [10,12], are here discussed, reviewing its relation to the net structure, particularly with transitions in the net that allow to increase/decrease the marking of a choice place. In Section 4, a homothecy property previously used for the analysis of CPN systems [13] is recalled; it is taken to prove that discontinuity of the equilibrium throughput implies its non-monotonicity. The relationships between these behaviors is provided for both the firing rate variation and the initial marking variation. In Section 5, taking inspiration from [4], undesired behaviors are related with net structural objects called *problematic configurations*. These objects have associated subnets in which the places do not contain the support of a P-semiflow. Finally, in Section 6, a set of reduction rules for simplifying the computation of problematic configurations is intuitively recalled by means of trivial cases. This procedure helps to practically diminish the complexity of the calculation, and more importantly, provides useful insights of the root of undesired behaviors.

2. Basic Concepts and Notations

Let $\mathbb{N}$, $\mathbb{Q}$, and $\mathbb{R}$ represent natural, rational, and real numbers, respectively. Given a set of numbers S, $S_{\geq 0}$ (resp. $S_{>0}$) denotes the set of nonnegative (resp. positive) numbers of S. Given a matrix M of size $|A| \times |B|$ with A and B sets of indices, the submatrix $M[A', B']$, with $A' \subset A$ and $B' \subset B$, denotes the restriction of M to rows indexed by A' and columns

indexed by B'. The support of a vector z is the set of indices corresponding to its non null values and is denoted by $\|z\|$.

2.1. Petri Net Structure and System

Definition 1. *A* Petri net structure *is a bipartite digraph defined by the four tuple* $N = \langle P, T, \textbf{Pre}, \textbf{Post} \rangle$, *where* $P \neq \emptyset$ *and* $T \neq \emptyset$ *are finite non-empty disjoint sets of nodes named* places *and* transitions, *respectively, and* $\textbf{Pre} : P \times T \to \mathbb{N} \cup \{0\}$ *($\textbf{Post} : P \times T \to \mathbb{N} \cup \{0\}$) is the* pre-incidence function *specifying the weighted arcs directed from places to transitions (*post-incidence function *that specifies the weighted arcs directed from transitions to places).*

A *subnet* of N, $N' = \langle P', T', \textbf{Pre}', \textbf{Post}' \rangle$, is a Petri net structure where $P' \subseteq P$, $T' \subseteq T$ are subsets of places and transitions of N, respectively; and $\textbf{Pre}' = \textbf{Pre}[P', T']$ and $\textbf{Post}' = \textbf{Post}[P', T']$ are the pre- and post-incidence functions of N restricted to P' and T'. The *preset* and *postset* of a node $v \in P \cup T$ are denoted as ${}^\bullet v$ (set of input nodes) and $v^\bullet$ (set of output nodes), respectively. These definitions can be naturally extended: let $V \subset P \cup T$ be a set of nodes, while ${}^\bullet V$ (respectively, $V^\bullet$) denotes the union of the preset (respectively, of the postset) of every node $v \in V$. A *siphon* is a set of places $\Sigma \subseteq P$ such that ${}^\bullet \Sigma \subseteq \Sigma^\bullet$.

The *token-flow* matrix (*incidence* matrix if the net is *self-loop free*) of a net N is defined as $C = \textbf{Post} - \textbf{Pre}$. A transition t_i with more than one input place (i.e., $|{}^\bullet t_i| > 1$) is named a join transition; a place p_j with more than one output transition (i.e., $|p_j^\bullet| > 1$) is named a choice place. A column vector $y \neq 0$ is called a *P-flow* of N if $y^T C = 0$; if the non-null entries of such vector are positive, then it is called a *P-semiflow*. A basis of the left kernel of C is a basis of P-flows and is denoted by B_y, so that $B_y^T C = 0$. Similarly, a column vector $x \neq 0$ is termed a *T-flow* of N if $Cx = 0$; if the non-null entries of that vector are positive, then it is termed a *T-semiflow*. If there is a P-semiflow (T-semiflow) such that $y > 0$ ($x > 0$), the net is said to be *conservative* (*consistent*), denoted as Cv (Ct).

Definition 2. *A net N is* Mono-T-Semiflow *(MTS) if it is conservative and consistent with a unique minimal (defined in the naturals, and least common multiple equals one) T-semiflow.*

2.2. Fluid or Continuous Petri Net System

A *marking* is a mapping $m : P \to \mathbb{R}_{\geq 0}^{|P|}$ that assigns to each place of N a non-negative real value.

Definition 3. *A* fluid or continuous Petri net *(CPN) system is a net N together with an* initial marking m_0, *and it is denoted as* $\langle N, m_0 \rangle$.

One characteristic of continuous Petri net systems is their evolution rule. It allows the firing of transitions in positive real amounts, while the reachable markings of the continuous system must be non-negative real values.

The *enabling degree* of a transition t at a marking m is defined as:

$$enab[t] = \min_{\forall p \in {}^\bullet t} \left\{ \frac{m[p]}{\textbf{Pre}[p, t]} \right\}. \tag{1}$$

A transition $t \in T$ is *enabled* if $enab[t] > 0$. An enabled transition can be *fired* in any real amount inside the interval $0 \leq \delta \leq enab[t]$. Its firing leads to a new marking $m' = m + \delta C[P, t]$. A marking m is *lim-reachable* from m_0 if there exists a (finite or infinite) firing sequence σ, such that m can be reached from m_0, which is denoted as $m_0[\sigma\rangle m$. A transition t is called *dead* if its enabling degree is zero ($enab[t] = 0$) for every reachable marking. The set of reachable markings, denoted as $RS(N, m_0)$, satisfy the following *fundamental* equation:

$$m = m_0 + C\sigma, \tag{2}$$

where $\sigma \in \mathbb{R}_{\geq 0}^{|T|}$ is the firing count vector of the sequence σ such that $m_0[\sigma\rangle m$.

Regarding Equation (2) and the P-flows of a net N, a *token conservation law* associated with a P-flow y is described by the equation $y^T m = y^T m_0$. This last equation is obtained by pre-multiplying Equation (2) by y^T.

Proposition 1 ([6,7]). *Let $\langle N, m_0 \rangle$ be a CPN system. If there is no empty siphon at m_0 and the net is consistent (not a real constraint in practical systems), then the following are equivalent:*

1. *The set of reachable markings;*
2. *The set of solutions of Equation (2), where $\sigma \geq 0$, $m \geq 0$;*
3. *The set of solutions of equation $B_y^T m = B_y^T m_0$, where $m \geq 0$.*

In this work, it is assumed that every system $\langle N, m_0 \rangle$ fulfils the previous condition: *there is no empty siphon at m_0 and the net is consistent*. If that is not the case, the places associated with the empty siphon, together with their output transitions, can be removed from the net because they never evolve.

In the case of continuous Petri net systems, the condition that there is not empty siphon at m_0 is equivalent to not having dead transitions in the CPN system.

Property 1. *Let $\langle N, m_0 \rangle$ be a consistent CPN system. There are no empty siphons at m_0 iff there are no dead transitions at m_0.*

Proof. (Sufficiency) If there are not dead transitions at m_0, then every transition in T can be fired at least once. Choose an arbitrary place p in an arbitrary siphon Σ; if p is marked at m_0, then the siphon Σ is marked at m_0. If p is not marked at m_0, then there should be a transition $t \in {}^\bullet p$ that can be fired, which means that all the places in ${}^\bullet t$ are marked; thus, the siphon Σ is marked at m_0. If that is not the case, this reasoning can be done upwards to find the place that marks the siphon, because every transition can be fired at least once.

(Necessity) If there are no empty siphons at m_0, then it is possible firing the enabled transitions (maybe in fractions of the enabling degree), so that new transitions are enabled maintaining the previous transitions enabled, which can be done until every place $p \in P$ is marked. Thus, every transition $t \in T$ can be fired. □

As a remark, the above property does not hold in both ways for discrete Petri nets. It is true that if there are not dead transitions at m_0, then there are no empty siphons at m_0. However, the converse is not true. Figure 3 shows a consistent Petri net with an initial marking: if considered as discrete, transition t_5 cannot be fired (it is a dead transition); however, there is no empty siphon at the initial marking. If considered as continuous, transition t_5 can be fired after firing transitions t_1 and t_2 by half its enabling degree.
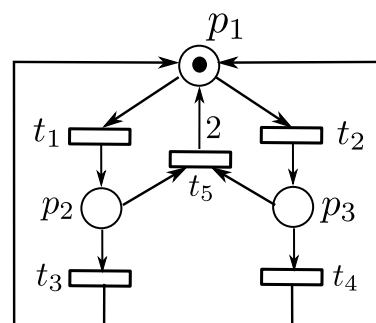

Figure 3. Consistent Petri net with no empty siphons. Transition t_5 is dead as discrete, but fireable as continuous.

Now, two algorithms are provided to evaluate the conditions: *there is no empty siphon at m_0* and *the net is consistent*.

Based on the results of [17], the Algorithm 1 determines if the net is consistent and has no dead transitions, which is equivalent to not having empty siphons in continuous Petri nets (Property 1). It computes if there is a T-semiflow $x \geq \mathbf{1}$ involving all transitions of the net N (line 2). If it exists, then it continues computing the set of enabled transitions at m_0 (line 8). Then, those transitions are fired with half their enabling degree (line 11) and the set of enabled transitions are computed again for the new marking (line 12). This procedure is repeated until the set of enabled transitions is T (there are no dead transitions) or the set does not grow anymore (there are dead transitions). The algorithm runs in polynomial time.

Algorithm 1 Computing if the net is consistent and there are no empty siphons at m_0.

Require: $\langle N, m_0 \rangle$.
Ensure: If N is consistent and there are no empty siphons
 1: Compute the token-flow matrix $C = \boldsymbol{Post} - \boldsymbol{Pre}$
 2: Compute the existence of a positive T-semiflow
    $\mathcal{P}_1 : \{$Find $x \geq \mathbf{1}$ s.t. $Cx = \mathbf{0}\}$
 3: **if** $\mathcal{P}_1$ has no solution **then**
 4:    N is not consistent
 5: **else**
 6:    N is consistent
 7:    $T^0 := \varnothing$
 8:    $T^1 := \{t | enab(t, m_0) > 0\}$
 9:    $j := 1$
 10:    **while** $T^j \neq T$ and $T^j \neq T^{j-1}$ **do**
 11:       Let σ_j be a sequence obtained firing all the transitions in $T^j \backslash T^{j-1}$ with half their enabling degree, and let $m_j := m_{j-1} + C\sigma_j$
 12:       $T^{j+1} := \{t | enab(t, m_j) > 0\}$
 13:       $j := j + 1$
 14:    **end while**
 15:    **if** $T^j = T$ **then**
 16:       There are no empty siphons at m_0
 17:    **else**
 18:       There are empty siphons at m_0
 19:    **end if**
 20: **end if**

Following the ideas in [2], another algorithm can be proposed to evaluate if there exists empty siphons at the initial marking. It consists of a linear algebraic method to obtain a *generating family* of siphons. Theorem 13 in [2] characterizes traps in terms of non-negative solutions to a linear of system inequalities. Siphons can be characterized in the same way by reversing the net. That theorem is now rewritten for siphons:

Theorem 1 ([2]). *Let* $N = \langle P, T, \boldsymbol{Pre}, \boldsymbol{Post} \rangle$ *be a Petri net. Define:*

$$N_\Sigma = \langle P, T, \boldsymbol{Pre}_\Sigma, \boldsymbol{Post} \rangle$$

such that $\boldsymbol{Pre}_\Sigma[p, t] = 0$ *if* $\boldsymbol{Pre}[p, t] = 0$, *and* $\boldsymbol{Pre}_\Sigma[p, t] = \Sigma_{p' \in t\bullet} \boldsymbol{Post}[p', t]$ *otherwise.*
A set $\Sigma \subseteq P$ *is a siphon of* N *iff* $y \geq \mathbf{0}$ *exists such that* $\|y\| = \Sigma$ *and* $y^T C_\Sigma \leq \mathbf{0}$.

Algorithm 2 decides if the net is consistent and there are no empty siphons at m_0. For this second condition, it computes a generating family of siphons for N. Then, it evaluates if there is an empty siphon at the initial marking.

Algorithm 2 Computing if the net is consistent and there are no empty siphons at m_0.

Require: $\langle N, m_0 \rangle$.
Ensure: If N is consistent and there are no empty siphons
1:   Compute the token-flow matrix $C = \boldsymbol{Post} - \boldsymbol{Pre}$
2:   Compute the existence of a positive T-semiflow
     $\mathcal{P}_{2-1} : \{ \text{Find } \boldsymbol{x} \geq \boldsymbol{1} \text{ s.t. } \boldsymbol{Cx} = \boldsymbol{0} \}$
3:   **if** $\mathcal{P}_{2-1}$ has no solution **then**
4:      N is not consistent
5:   **else**
6:      N is consistent
7:      Construct N_Σ for N as in Theorem 1
8:      Find an unmarked siphon:
        $\mathcal{P}_{2-2} : \{ \text{Find } \boldsymbol{y} \geq \boldsymbol{0} \text{ s.t. } \boldsymbol{y}^T \boldsymbol{C}_\Sigma \leq \boldsymbol{0} \wedge \boldsymbol{y}^T \boldsymbol{m}_0 = \boldsymbol{0} \}$
9:      **if** $\mathcal{P}_{2-2}$ has a solution **then**
10:        There is at least one empty siphon at m_0
11:      **else**
12:        There are no empty siphons at m_0
13:      **end if**
14: **end if**

2.3. Timed Continuous Petri Net Systems

If the firing of transitions is timed, the marking of the continuous system evolves deterministically along a trajectory within the set of reachable markings. In this sense, Equation (2) depends explicitly on time (that is, $\boldsymbol{m}(\tau) = \boldsymbol{m}_0 + \boldsymbol{C}\boldsymbol{\sigma}(\tau)$), and its time derivative gives the *state equation*:

$$\dot{\boldsymbol{m}}(\tau) = \boldsymbol{C}\dot{\boldsymbol{\sigma}}(\tau), \quad m(0) = m_0. \tag{3}$$

The derivative of the firing count vector is known as the *firing flow* or *throughput* vector of the timed model $\boldsymbol{f}(\tau) = \dot{\boldsymbol{\sigma}}(\tau)$. As already pointed out, in this work, the firing flow is defined using the *infinite servers semantics* [6,7]:

$$\boldsymbol{f}[t_j] = \boldsymbol{\lambda}[t_j] \min_{\forall p \in {}^\bullet t_j} \left\{ \frac{\boldsymbol{m}[p]}{\boldsymbol{Pre}[p, t_j]} \right\}, \tag{4}$$

where $\boldsymbol{\lambda} : T \to \mathbb{Q}_{>0}^{|T|}$ is a mapping known as the *firing rate* vector, which assigns to each transition of N a positive real value.

The firing flow represents the number of transition firings per unit time, i.e., the throughput of the transition. Given a net structure, according to previous equation, it depends on two sets of parameters that may be tuned: the firing rate vector $\boldsymbol{\lambda}$ and the current marking $\boldsymbol{m}$. Defined by $Pre[p, t_j]$ and $Post[p, t_j]$, the structure of the net plays a key role in the possible evolution of the flow, being able to introduce undesirable behaviors (such as non-monotonicity in the equilibrium throughput). In Section 5, structural objects denoted as *problematic* configurations are used to explain these undesirable behaviors. Notice that both $\boldsymbol{\lambda}$ and $\boldsymbol{m}$ directly affect the flow, so it suggests a "kind of duality". However, this duality is a *weak* one, since $\boldsymbol{\lambda}$ is a fixed timed net parameter, while $\boldsymbol{m}$ is changing during the net system evolution. The following sections show the scope of such a duality.

Definition 4. *A timed continuous Petri net (TCPN) system is a CPN system together with a firing rate vector $\boldsymbol{\lambda}$ and it is denoted as $\langle N, \boldsymbol{\lambda}, m_0 \rangle$.*

Due to the min operator in Equation (4) and the token conservation laws, the marking evolution of a TCPN system can be represented by an *affine positive piecewise linear system* [6]. The following concepts are useful to study their structure and behaviors:

1. A *configuration* $\mathcal{C}$ of a net N is a set of (p, t) arcs, only one per each transition, such that $p \in {}^\bullet t$. The *T-coverture* of a configuration $\mathcal{C}$ is $\mathcal{T}_\mathcal{C} = \{p \mid \forall t \in T, (p, t) \in \mathcal{C}\}$, i.e., the places preceding the arcs of $\mathcal{C}$.

2. A configuration $\mathcal{C}$ has associated a *configuration matrix* $\boldsymbol{\Pi}_\mathcal{C} \in \mathbb{Q}_{\geq 0}^{|T| \times |P|}$ where:

$$\boldsymbol{\Pi}_\mathcal{C}[t_j, p_i] = \begin{cases} \dfrac{1}{\boldsymbol{Pre}[p_i, t_j]} & \text{if } (p_i, t_j) \in \mathcal{C} \\ 0 & \text{otherwise.} \end{cases} \tag{5}$$

A configuration $\mathcal{C}$ is *active* at marking $\boldsymbol{m}$ if $\boldsymbol{\Pi}_\mathcal{C} \boldsymbol{m} = \boldsymbol{enab}(\boldsymbol{m})$ (i.e., if their arcs are constraining the flow of transitions).

3. A *region* $\mathcal{R}_\mathcal{C}$ is a (sub)state space in which a unique configuration $\mathcal{C}$ is active. Regions constitute a partition—except on the borders—of the full polytope (possibly unbounded) of reachable markings.

4. The *associated net* of a configuration $\mathcal{C}$ is defined as the subnet $N_\mathcal{C} = (\mathcal{T}_\mathcal{C}, \mathcal{T}_\mathcal{C}^\bullet, \boldsymbol{Pre}', \boldsymbol{Post}')$.

5. An *operation mode* or *regime* $\Sigma_\mathcal{C}$ of a TCPN system is the linear system ($\dot{\boldsymbol{m}} = \boldsymbol{C}\boldsymbol{\Lambda}\boldsymbol{\Pi}_\mathcal{C} \boldsymbol{m}$, where $\boldsymbol{\Lambda} = diag(\boldsymbol{\lambda})$ is a diagonal matrix) which describes the marking evolution, while $\boldsymbol{m}$ evolves within region $\mathcal{R}_\mathcal{C}$. At configuration $\mathcal{C}$, $\boldsymbol{C}\boldsymbol{\Lambda}\boldsymbol{\Pi}_\mathcal{C}$ is the *dynamic matrix*.

The set of all configurations of a net N is represented as $SC(N)$, its number being bounded by $\Pi_i |{}^\bullet t_i|$. Therefore, a net may contain an exponential number of configurations. As a notation, $\mathcal{C}_{i_1, \dots, i_{|T|}}$ is a configuration where $(p_{i_k}, t_k) \in \mathcal{C}_{i_1, \dots, i_{|T|}}$. Figure 1b has $\Pi_i |{}^\bullet t_i| = 2 \times 2 \times 2 \times 2 \times 2 \times 2 \times 1 = 64$ different configurations. In Figure 4, we are depicting the induced subnets by four of them.
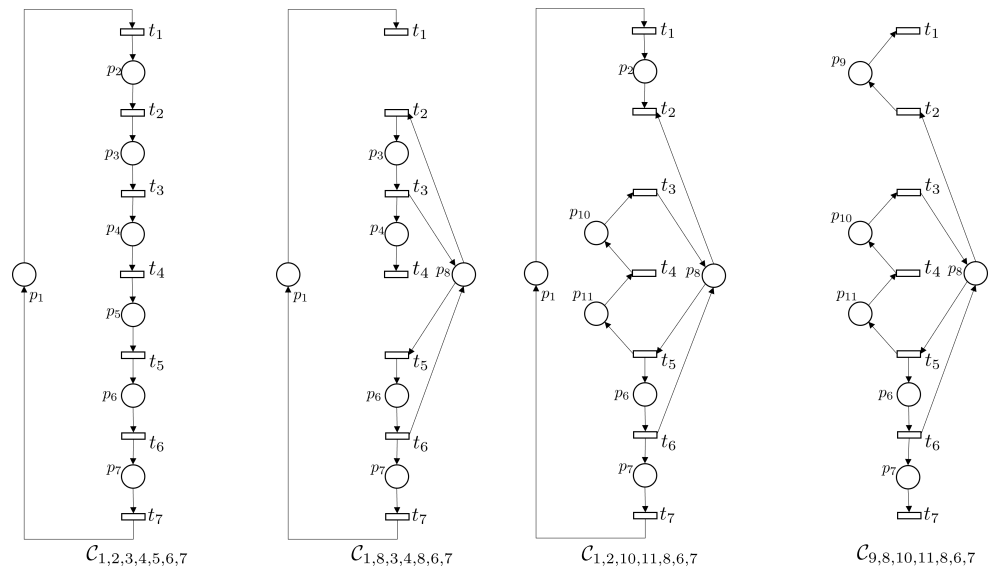
Figure 4. Induced nets associated with 4 of the 64 configurations of the net depicted in Figure 1b.

The dynamic behavior of a TCPN system can be described by the following equations:

$$\begin{aligned} \dot{\boldsymbol{m}} &= \boldsymbol{C}\boldsymbol{\Lambda}\boldsymbol{\Pi}_\mathcal{C} \boldsymbol{m}, \quad \boldsymbol{m} \in \mathcal{R}_\mathcal{C}, \quad \mathcal{C} \in SC(N) \\ \boldsymbol{m}(0) &= \boldsymbol{m}_0. \end{aligned} \tag{6}$$

Configurations and T-covertures are sets related with the structure of the net N. Both structural objects allow to address some analysis of the system and are key for the results presented in upcoming sections. They are also related to the regions of the CPN system $\langle N, \boldsymbol{m}_0 \rangle$ and to the operation modes of the TCPN system $\langle N, \boldsymbol{\lambda}, \boldsymbol{m}_0 \rangle$.

An *equilibrium marking* $\boldsymbol{m}_e \in \mathcal{R}_\mathcal{C}$ is a state of the TCPN system fulfilling $\dot{\boldsymbol{m}} = \boldsymbol{C}\boldsymbol{\Lambda}\boldsymbol{\Pi}_\mathcal{C} \boldsymbol{m}_e = \boldsymbol{0}$; its corresponding *equilibrium throughput* is denoted by $f_e = \boldsymbol{\Lambda}\boldsymbol{\Pi}_\mathcal{C} \boldsymbol{m}_e$.

Note that $\Lambda \geq \mathbf{0}$, $\Pi_{\mathcal{C}} \geq \mathbf{0}$ and $m_e \geq \mathbf{0}$, and thus, $f_e \geq \mathbf{0}$, and it is a non-negative linear combination of the T-semiflows of the net, no matter which configuration is activated by m_e.

2.4. Mono-T-Semiflow Nets and Performance Properties Relationships

The equilibrium throughput, in the case of MTS systems, is proportional to the unique T-semiflow of the net. Thus, it can be expressed as:

$$f_e = \Lambda \Pi_{\mathcal{C}} m_e = \alpha x,$$

where x is the T-semiflow of the net and $\alpha(N, \lambda, m_0)$ is a scalar function. In other words, the equilibrium throughput is of the form $f_e(N, \lambda, m_0)$.

The dynamic behavior of a TCPN system is described by Equations (4) and (6). From them, it can be directly derived that, since the dynamic behavior of a TCPN system can be described by Equation (6)—the marking evolution of $\langle N, \lambda, m_0 \rangle$ is the solution to that initial value problem—the following well known *homothecy* properties are dynamically satisfied [6]:

- If m_0 is multiplied by a constant $k > 0$, the reachable markings are multiplied by k and the firing flow will also be k times bigger (or smaller if $k < 1$).
- If λ is multiplied by a constant $k > 0$, then identical markings will be reached, but the system will evolve k times faster (or slower if $k < 1$).

We emphasize that in both cases, the whole m_0 and λ are multiplied by k. However, when the value of only one entry of these vectors varies, then the equilibrium throughput could exhibit paradoxical behaviors. This case is analyzed in this work.

3. Bifurcations: Operation Mode Properties

The equilibrium throughput $f_e = \Lambda \Pi_{\mathcal{C}} m_e$ depends on the transition firing rate Λ, the structure of the net $\Pi_{\mathcal{C}}$, and the equilibrium marking m_e. Now, we illustrate how the behavior of the equilibrium marking of $\dot{m} = C\Lambda\Pi_{\mathcal{C}} m$ changes in a given region when the transition speed (firing rate or throughput of the machines) varies. In order to do that, a similarity transformation is used to split $C\Lambda\Pi_{\mathcal{C}}$ into the non-zero and zero eigenvalue parts. It easily shows how bifurcations are generated. These concepts are illustrated through examples. Finally, a discussion for a subclass of nets is addressed.

3.1. A Transformation for the Bifurcation Analysis

Unfortunately, as mentioned before, varying the production throughput of machines may lead to paradoxical throughput behaviors of the system, in which the increment of speed of machines or system resources leads to the decrease of the system throughput or abrupt changes of it, even leading to deadlocks. This can be explained using bifurcations.

A *bifurcation* of an equilibrium marking takes place when a change of the system parameters produces a change of the qualitative behavior of the equilibrium marking (see references [14,18] for technical details). For instance, due to the variation of a firing rate (a parameter of the dynamic matrices of a TCPN system), the equilibrium marking can pass from stable to unstable. This can be verified using the eigenvalues of the dynamic matrices $C\Lambda\Pi_{\mathcal{C}}$ and observing their relocation from the left half complex plane to the right half complex plane.

The conservation marking laws imposed by the P-flows fix some eigenvalues to zero, making them independent from firing rate variations. Thus, the equilibrium marking bifurcation analysis may be performed on a reduced matrix, where the zero eigenvalues are not considered. This can be easily done by using the following *similarity* transformation [14]:

$$T = \begin{bmatrix} T_1 \\ B_y{}^T \end{bmatrix}, \tag{7}$$

where B_y is a matrix composed of a basis of the P-flows and T_1 is an adequate matrix, such that T is invertible, and $T^{-1} = \begin{bmatrix} z_1 & z_y \end{bmatrix}$.

Hence, the coordinate change is $\bar{m} = Tm$ and the marking derivative in the new coordinates is:

$$\dot{\bar{m}} = TC\Lambda\Pi_k T^{-1}\bar{m},$$

and can be decomposed as:

$$\begin{bmatrix} \dot{\bar{m}}_1 \\ \dot{\bar{m}}_y \end{bmatrix} = \begin{bmatrix} T_1 C\Lambda\Pi_k z_1 & T_1 C\Lambda\Pi_k z_y \\ 0 & 0 \end{bmatrix} \begin{bmatrix} \bar{m}_1 \\ \bar{m}_y \end{bmatrix}. \tag{8}$$

According to this transformation, the eigenvalues of $T_1 C\Lambda\Pi_k z_1$ are those of $C\Lambda\Pi_k$ not associated with the P-flows. Now, this *reduced system* $T_1 C\Lambda\Pi_k z_1$ is used to study if a loss of hyperbolicity occurs by varying the firing rates λ. The following definition provides a formal statement of these concepts.

Definition 5 ([14]). *An equilibrium marking, $m_e \in \mathcal{R}_C$, is said to be* hyperbolic *if none of the eigenvalues of the dynamic matrix $C\Lambda\Pi_C$ lie on the imaginary axis. The equilibrium marking* bifurcates *when, due to varying a parameter $\lambda[t_j] = \lambda_j$, it loses hyperbolicity.*

Varying the firing rates of transitions, it is possible to change the eigenvalues of $T_1 C\Lambda\Pi_k z_1$. If the system loss hyperbolicity, a change in the qualitative behavior of the system occurs.

For instance, if the marking of a TCPN system is evolving in a region in which all the eigenvalues of the dynamic matrix (different from the associated with P-semiflows) have a negative real part, the marking will reach zero if it evolves in the same region, reaching a deadlock in the system. A slight variation of the firing rates can change this behavior, so that one of the eigenvalues relies on the imaginary axis. The marking evolving in such region cannot reach zero, thus the equilibrium throughput of the system will be different from zero. Moreover, that slight variation can change one of the eigenvalues, so that its real part is positive. The marking evolving in such a region will increase its value until it reaches another region (if the system is bounded). This is why we can see *jumps* in the equilibrium throughput due to the firing rate variations.

3.2. Bifurcations in a Manufacturing TCPN Model

Let us introduce intuitively the idea of bifurcation. There can exist path losing/gaining marks when considering a subnet associated with an operation mode. For instance, the places of the subnet in Figure 5a lose markings if t_2 is fired, while their marking is increased by firing t_5, t_4, and t_3, in that order. As mentioned in Section 2, every operation mode of a TCPN is a linear system $\dot{m} = C\Lambda\Pi_C m$. Depending on the existence of path losing/gaining marks, the firing rates of transitions may be changed to obtain a stable/unstable linear system. For example, considering the net depicted in Figure 1b, one of its configurations, its associated subnet, and its dynamic matrix are depicted in Figure 5.

The dynamic matrix of the operation mode associated with the configuration is $A_C = C\Lambda\Pi_C$ and it is depicted in Figure 5b, where $\lambda(t_2) = \lambda_2$ is considered as a parameter. Notice that in the subnet shown in Figure 5a, for example, the total marking is decremented by the firing of t_2 and increased by the firing of t_5. In the following lines, we explain how this phenomenon is captured by A_C.

$$A_{\mathcal{C}} = \begin{bmatrix} -1 & 0 & 0 & 0 & 0 & 0 & 1 & 0 & 0 & 0 & 0 & 0 \\ 1 & 0 & 0 & 0 & 0 & 0 & 0 & -\lambda_2 & 0 & 0 & 0 & 0 \\ 0 & 0 & 0 & 0 & 0 & 0 & 0 & \lambda_2 & 0 & -1 & 0 & 0 \\ 0 & 0 & 0 & 0 & 0 & 0 & 0 & 0 & 0 & 1 & -1 & 0 \\ 0 & 0 & 0 & 0 & 0 & 0 & 0 & -1 & 0 & 0 & 1 & 0 \\ 0 & 0 & 0 & 0 & 0 & -1 & 0 & 1 & 0 & 0 & 0 & 0 \\ 0 & 0 & 0 & 0 & 0 & 1 & -1 & 0 & 0 & 0 & 0 & 0 \\ 0 & 0 & 0 & 0 & 0 & 1 & 0 & -\lambda_2 & -1 & 0 & 1 & 0 & 0 \\ -1 & 0 & 0 & 0 & 0 & 0 & 0 & \lambda_2 & 0 & 0 & 0 & 0 \\ 0 & 0 & 0 & 0 & 0 & 0 & 0 & 0 & 0 & -1 & 1 & 0 \\ 0 & 0 & 0 & 0 & 0 & 0 & 0 & 1 & 0 & 0 & -1 & 0 \\ 0 & 0 & 0 & 0 & 0 & -1 & 1 & 0 & 0 & 0 & 0 & 0 \end{bmatrix}$$

Figure 5. Subnet of configuration $\mathcal{C}_{1,8,10,11,8,6,7}$ of the TCPN model of Figure 1b and the dynamic matrix of its associated operation mode. (**a**) Subnet. (**b**) Dynamic Matrix.

Matrix $A_{\mathcal{C}}$ has six eigenvalues associated with a basis of P-flows of the net (in this particular case, they are P-semiflows of the net). Of course, all these are independent from λ_2 and are equal to zero. A similarity transformation T to obtain a transformed matrix $TA_{\mathcal{C}}T^{-1}$ for the analysis of the remaining eigenvalues is the following. Note that the last six rows are (transposed) minimal P-semiflows of the net.

$$T = \begin{bmatrix} I_6 & 0_6 \\ B_y^T \end{bmatrix} = \begin{bmatrix} 1 & 0 & 0 & 0 & 0 & 0 & 0 & 0 & 0 & 0 & 0 & 0 \\ 0 & 1 & 0 & 0 & 0 & 0 & 0 & 0 & 0 & 0 & 0 & 0 \\ 0 & 0 & 1 & 0 & 0 & 0 & 0 & 0 & 0 & 0 & 0 & 0 \\ 0 & 0 & 0 & 1 & 0 & 0 & 0 & 0 & 0 & 0 & 0 & 0 \\ 0 & 0 & 0 & 0 & 1 & 0 & 0 & 0 & 0 & 0 & 0 & 0 \\ 0 & 0 & 0 & 0 & 0 & 1 & 0 & 0 & 0 & 0 & 0 & 0 \\ \hline 0 & 1 & 0 & 0 & 0 & 0 & 0 & 0 & 1 & 0 & 0 & 0 \\ 0 & 0 & 0 & 1 & 0 & 0 & 0 & 0 & 0 & 1 & 0 & 0 \\ 0 & 0 & 0 & 0 & 1 & 0 & 0 & 0 & 0 & 0 & 1 & 0 \\ 0 & 0 & 1 & 0 & 0 & 1 & 0 & 1 & 0 & 0 & 0 & 0 \\ 0 & 0 & 0 & 0 & 0 & 0 & 1 & 0 & 0 & 0 & 0 & 1 \\ 1 & 1 & 1 & 1 & 1 & 1 & 1 & 0 & 0 & 0 & 0 & 0 \end{bmatrix}$$

$$TA_{\mathcal{C}}T^{-1} = \begin{bmatrix} -2 & -1 & -1 & -1 & -1 & -1 & 0 & 0 & 0 & 0 & 0 & 1 \\ 1 & 0 & \lambda_2 & 0 & 0 & \lambda_2 & 0 & 0 & 0 & -\lambda_2 & 0 & 0 \\ 0 & 0 & -\lambda_2 & 1 & 0 & -\lambda_2 & 0 & -1 & 0 & \lambda_2 & 0 & 0 \\ 0 & 0 & 0 & -1 & 1 & 0 & 0 & 1 & -1 & 0 & 0 & 0 \\ 0 & 0 & 1 & 0 & -1 & 1 & 0 & 0 & 1 & -1 & 0 & 0 \\ 0 & 0 & -1 & 0 & 0 & -2 & 0 & 0 & 0 & 1 & 0 & 0 \\ \hline 0 & 0 & 0 & 0 & 0 & 0 & 0 & 0 & 0 & 0 & 0 & 0 \\ 0 & 0 & 0 & 0 & 0 & 0 & 0 & 0 & 0 & 0 & 0 & 0 \\ 0 & 0 & 0 & 0 & 0 & 0 & 0 & 0 & 0 & 0 & 0 & 0 \\ 0 & 0 & 0 & 0 & 0 & 0 & 0 & 0 & 0 & 0 & 0 & 0 \\ 0 & 0 & 0 & 0 & 0 & 0 & 0 & 0 & 0 & 0 & 0 & 0 \\ 0 & 0 & 0 & 0 & 0 & 0 & 0 & 0 & 0 & 0 & 0 & 0 \end{bmatrix}$$

In order to obtain the eigenvalues of the transformed matrix, the characteristic polynomial of $TA_{\mathcal{C}}T^{-1}$ is obtained:

$$P(s) = s^6(s^6 + (\lambda_2 + 6)s^5 + (5\lambda_2 + 14)s^4 + (10\lambda_2 + 15)s^3 + (10\lambda_2 + 6)s^2 + (5\lambda_2 - 1)s + (\lambda_2 - 1))$$

The eigenvalues of the transformed matrix are the roots of $P(s)$. Obviously, the transformed matrix has six eigenvalues equal to zero ($s = 0$), as expected, and they do not depend on λ_2. Moreover, $P(s)$ can be factorized as follows:

$$P(s) = s^6(s+1)^3(s^3 + (\lambda_2 + 3)s^2 + (2\lambda_2 + 2)s + \lambda_2 - 1).$$

Hence, there are three other eigenvalues that do not depend on λ_2, and they have the same value $s = -1$. One of these eigenvalues is due to the firing rate of transition t_1 ($\lambda_1 = 1$), which determines the velocity of the marking evolution of p_1. In the same way, the firing rate of transition t_7 ($\lambda_7 = 1$) gives another eigenvalue in $s = -\lambda_7 = -1$.

The other three non-zero eigenvalues depend on the parameter λ_2 (the speed of retrieving a part). In Figure 6, the variation of these three last eigenvalues is depicted. In this case, $\lambda_2 \in (0, 10]$. The starting roots (when $\lambda_2 = 0$) are represented by symbol 'X', while the endings (when $\lambda_2 = 10$) are represented by symbol 'O'. If we increase λ_2 indefinitely, that is $\lambda_2 \to \infty$, one of the eigenvalues will increase ($s \to -\infty$) indefinitely, and the other two will tend to $s = -1$ (this is obtained dividing $s^3 + (\lambda_2 + 3)s^2 + (2\lambda_2 + 2)s + \lambda_2 - 1 = 0$ by λ_2 and obtaining the limit when $\lambda_2 \to \infty$). Notice that:

- If $\lambda_2 < 1$, the equilibrium marking is hyperbolic (eigenvalues are not on the imaginary axis), and there exists one eigenvalue of $A_{\mathcal{C}}$ located in the right part of the complex plane, that is, the equilibrium marking of the reduced system is unstable within that region. The marking of the T-coverture increases until it reaches another region, activating another configuration.
- If $\lambda_2 = 1$, then the previous eigenvalue on the right part of the complex plane is relocated to the imaginary axis of the complex plane (a new zero eigenvalue); thus, the reduced system is non-hyperbolic and, in this case, critically stable.
- If $\lambda_2 > 1$, then the eigenvalue goes to the left part of complex plane, and thus, the equilibrium marking becomes hyperbolic and stable, and the marking of the reduced system evolves until it reaches a deadlock.
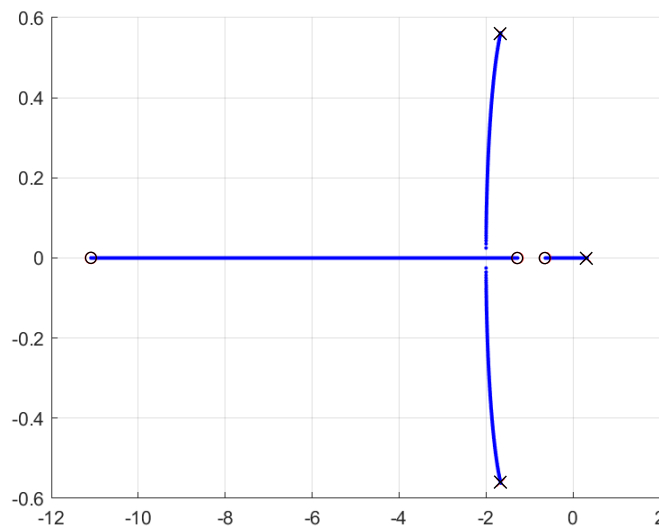

Figure 6. Location of three of the eigenvalues of matrix $A_{\mathcal{C}}$ on the complex plane when λ_2 is varied from zero to ten. When λ_2 is close to zero, the eigenvalues are located on the 'X' symbol. By increasing λ_2, the eigenvalues move through the blue line until they reach the 'O' symbol, where the value of λ_2 is ten.

Consequently, a *bifurcation* occurs for $\lambda_2 = 1$. According to [12], this marking bifurcation explains the discontinuity of the equilibrium throughput with respect to the firing rate t_2, which can be seen in Figure 2b.

3.3. Bifurcations in Timed Join Free and Choice Free Nets

In a Join Free TCPN (JF TCPN), every transition has only one input place ($\forall t \in T$, $|{}^{\bullet}t| = 1$); thus, JF TCPNs have only one configuration. In a Choice Free TCPN (CF TCPN), every place has only one output transition ($\forall p \in P, |p^{\bullet}| = 1$); thus, CF TCPNs have no decision places. If the net is Join-Free (JF) or Choice-Free (CF), bifurcations of the equilibrium marking cannot occur in the TCPN system when the nets are consistent and conservative [14].

Bifurcations of the equilibrium marking in strongly connected JF TCPN systems may appear due to the variation of some firing rates. As already said, that will be reflected in the eigenvalues of its *unique* dynamic matrix $C\Lambda\Pi$. Let us illustrate this through the following example, in which the equilibrium marking of the system changes from being unstable to stable.

Example 1. *Consider the JF TCPN in Figure 7a with $\lambda = \begin{bmatrix} \lambda_1 & 1 & 1 & 1 \end{bmatrix}^T$ and $m_0 = \begin{bmatrix} 10 & 0 & 0 \end{bmatrix}^T$. It is strongly connected and consistent, but non-conservative (in fact, it has no P-semiflows). Its unique dynamic matrix is:*

$$A = C\Lambda\Pi = \begin{bmatrix} -\lambda_1 - 1 & 0.5 & 2 \\ \lambda_1 & -1 & 0 \\ 1 & 0 & -1 \end{bmatrix}.$$

- *If $0 < \lambda_1 < 2$, then A is a full rank matrix, so none of its eigenvalues rely on the imaginary axis (i.e., the only equilibrium marking, $m_e = 0$, is hyperbolic). In this case, one of them has a positive real part; thus, m_e is unstable.*
- *If $\lambda_1 = 2$, then A is singular, and one of its eigenvalues is zero. That is, the equilibrium marking ($m_e = \beta \begin{bmatrix} 1 & 2 & 1 \end{bmatrix}^T$, with $\beta \geq 0$) is non-hyperbolic.*
- *If $\lambda_1 > 2$, then A is a full rank matrix, so $m_e = 0$ is hyperbolic. Specifically, all the eigenvalues have a negative real part; m_e is stable.*
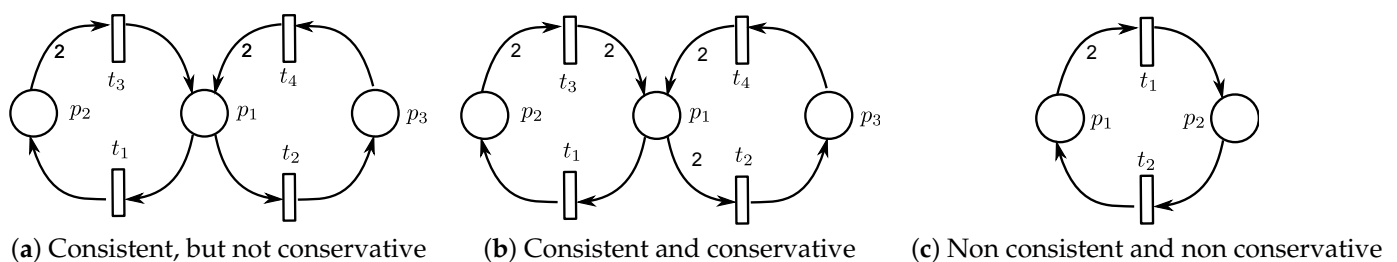
Consequently, a bifurcation occurs for $\lambda_1 = 2$.

(**a**) Consistent, but not conservative   (**b**) Consistent and conservative   (**c**) Non consistent and non conservative

Figure 7. Three strongly connected JF Petri nets: (**a**) its TCPN system exhibits bifurcations; (**b**,**c**): their TCPN systems do not exhibit bifurcations.

Nevertheless, if the JF TCPN is conservative, a bifurcation of the equilibrium markings is not possible. It follows from the fact that it cannot have closed paths gaining/losing tokens.

Proposition 2 ([14])**.** *Let (N, λ, m_0) be a strongly connected JF TCPN system. If N has a P-semiflow, then the equilibrium markings of the system do not bifurcate.*

The equilibrium markings of the TCPN system (N, λ, m_0) for the net in Figure 7b do not bifurcate, because N is consistent and conservative (therefore, structurally live).

The converse of Proposition 2 is not true; consider the net in Figure 7c. For every $\lambda > 0$ the dynamic matrix of the TCPN system, $A = C\Lambda\Pi$, has only eigenvalues with a negative real part. Therefore, $m_e = 0$ is always hyperbolic; thus, there is no bifurcation value for any $\lambda > 0$, and the net has no P-semiflow.

When the assumption of strongly connectedness is removed in Proposition 2, N must be conservative to guarantee that the equilibrium markings of the reduced subsystem do not bifurcate. This is because if N is not strongly connected and conservative, then it should be not consistent (this is a classical result: Ct & Cv imply strongly connectedness of the net [2]). Hence, the net is not structurally live, which guarantees that the eigenvalues of the reduced system are in the left half of the complex plane.

Similarly, strongly connected (and thereby conservative) CF TCPN do not exhibit bifucations. The next proposition formalizes this fact.

Proposition 3 ([14]). *Let* (N, λ, m_0) *be a strongly connected CF TCPN system. If N has a T-semiflow, then the equilibrium markings of the system do not bifurcate.*

Bifurcations, as well as deadlocks (reviewed in the following sections), are not possible in CF and JF TCPN, which are consistent and conservative. This relationship is due to the fact that P-semiflows are contained in the places associated with every configuration of the net.

4. Discontinuities and Non-Monotonicities

Section 3 illustrated the fact that bifurcations are the responsible of discontinuities in the equilibrium marking when the firing rates varies. In fact, here we focus on the idea that discontinuities imply non-monotonicities. Based on the homothecy property, it is shown how a discontinuity in the equilibrium throughput implies a non-monotonicity, either with respect to a firing rate or initial marking variations.

4.1. The Firing Rate Variation Case

In order to provide a formal definition of discontinuities and non-monotonicities, some definitions are given. They capture possible equilibrium throughput changes when the firing rates vary. In the following properties of the equilibrium throughput, the initial marking m_0 is fixed and the firing speed of transitions λ varies. Some kind of "dual" properties, fixing λ and varying m_0 can be established [15].

Definition 6. *Let* $\langle N, \lambda, m_0 \rangle$ *be a TCPN system with* m_0 *fixed. Assume that the firing rate vector* λ *is arbitrary. Its equilibrium throughput is:*

- *Monotonic with respect to the firing rates, denoted as $M(\lambda)$, if $\forall(\lambda, \lambda')$, $\lambda \leq \lambda' \implies \alpha(\lambda) \leq \alpha(\lambda')$;*
- *Deadlock-free monotonic with respect to the firing rates, denoted as $DFM(\lambda)$, if $\forall(\lambda, \lambda')$ with $\lambda \leq \lambda'$, $\alpha(\lambda) > 0 \implies \alpha(\lambda') > 0$,*
- *Continuous with respect to the firing rates, denoted as $C(\lambda)$, if for every λ, given $\epsilon > 0$, there is $\delta > 0$, such that $\|\lambda - \lambda'\|_2 < \delta \implies \|\alpha(\lambda) - \alpha(\lambda')\|_2 < \epsilon$, where $\|\cdot\|_2$ is the euclidean norm.*

The following example shows a firing rate variation in an MTS-TCPN, which leads to discontinuous changes in the equilibrium throughput, similar to the discontinuous change observed in Figure 2b. Then, it is illustrated how a discontinuous change implies non-monotonicity. In order to simplify the explanation, the apparently simple TCPN system of Figure 8 with only four configurations is used. The configurations of this net are: $\mathcal{C}_{1,1}$, $\mathcal{C}_{2,1}$, $\mathcal{C}_{1,3}$, and $\mathcal{C}_{2,3}$. The same property can be observed for the net model in Figure 1b; however, for the sake of simplicity, it is not used in this case.
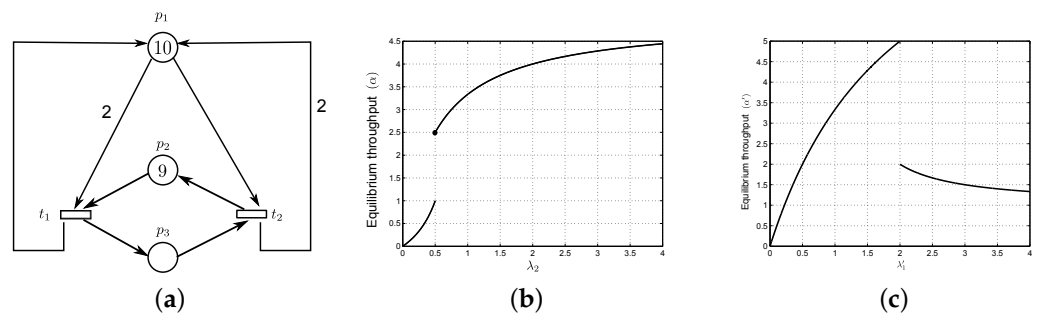
Figure 8. An MTS net, its equilibrium throughput when λ_2 varies (Figure 8b), and its equilibrium throughput when λ_1 varies (Figure 8c). Note that the first one is monotone and the last one is non-monotone. (**a**) An MTS net. The firing of t_1 reduces the tokens in p_1, while the firing of t_2 increases its value. (**b**) Equilibrium throughput with respect to λ_2 of the net system in Figure 8a. (**c**) Equilibrium throughput with respect to λ_1' constructed using the time-scale property. A non-monotonicity is discovered from a discontinuity in the equilibrium throughput.

Consider the MTS net in Figure 8a with an initial marking $m_0 = \begin{bmatrix} 10 & 9 & 0 \end{bmatrix}^T$ and firing rates $\lambda = \begin{bmatrix} 1 & \lambda_2 \end{bmatrix}^T$, where λ_2 is taken as a variation parameter. The net has two minimal P-semiflows $y_1 = \begin{bmatrix} 1 & 0 & 1 \end{bmatrix}^T$ and $y_2 = \begin{bmatrix} 0 & 1 & 1 \end{bmatrix}^T$ (hence, $m_1 + m_3 = 10$ and $m_2 + m_3 = 9$) and only one minimal T-semiflow $x = \begin{bmatrix} 1 & 1 \end{bmatrix}^T$.

Since the net is an MTS-TCPN, the equilibrium throughput of the system is $f_e = \Lambda \Pi_C m_e = \alpha x$. Table 3 shows the value of the equilibrium throughput, for some intervals of λ_2, in which a discontinuity of the equilibrium throughput is observed.

Table 3. Equilibrium throughput w.r.t. λ_2 and its characteristics of the MTS net depicted in Figure 8a.

	Equilibrium Throughput w.r.t. λ_2		
λ_2 **Interval**	**Equilibrium Throughput** f_e	m_e **Activates Configuration:**	m_e **Belongs to Region:**
$0 < \lambda_2 < 0.5$	$\alpha = \dfrac{\lambda_2}{1 - \lambda_2}$	$\mathcal{C}_{21} = (p_2, t_1), (p_1, t_2)$	$\mathcal{R}_{21}$
$\lambda_2 = 0.5$	$\alpha = 2.5$	$\mathcal{C}_{11} = (p_1, t_1), (p_1, t_2)$ and $\mathcal{C}_{13} = (p_1, t_1), (p_3, t_2)$	$\mathcal{R}_{11} \cap \mathcal{R}_{13}$
$\lambda_2 > 0.5$	$\alpha = \dfrac{10\lambda_2}{1 + 2\lambda_2}$	$\mathcal{C}_{13} = (p_1, t_1), (p_3, t_2)$	$\mathcal{R}_{13}$

In this case, the discontinuity can be explained due to the bifurcation that occurs when $\lambda_2 = 0.5$. The linear system which determines the marking evolution when place p_1 restricts the firing of t_1 and t_2 is: unstable if $\lambda_2 < 0.5$; critically stable if $\lambda_2 = 0.5$; and stable if $\lambda_2 > 0.5$. The loss of hyperbolicity in this case (bifurcation) produces a discontinuity in the equilibrium throughput.

Despite the discontinuity at $\lambda_2 = 0.5$, Figure 8b shows that the equilibrium throughput is monotone with respect to λ_2 variations. In order to show the non-monotonicity of this system, the equilibrium throughput, when λ_1 varies, is obtained using λ_2 as a parameter and the homothecy properties. Now, the equilibrium throughput f_e' is computed for the above TCPN as a function of f_e when $\lambda' = k\lambda$ and $k = 1/\lambda_2$.

Let us use the previous calculations of the TCPN system in Figure 8b. Consider point A' in Figure 9; it is in the line that represents vector $\lambda = \begin{bmatrix} 1 & \lambda_2 \end{bmatrix}^T$ for interval $0 < \lambda_2 < 0.5$; the equilibrium throughput $f_e = \alpha_{A'} x$ for this interval is described by $\alpha_{A'} = \dfrac{\lambda_2}{1 - \lambda_2}$. Now consider point A is on the line that represents vector $\lambda' = \begin{bmatrix} \lambda_1' & \lambda_2' \end{bmatrix}^T = \begin{bmatrix} \dfrac{1}{\lambda_2} & 1 \end{bmatrix}^T = k\lambda$,

where $k = \dfrac{1}{\lambda_2}$, for the interval $\lambda_1' > 2$. Hence, now the equilibrium throughput is described

by $\alpha_A = k\alpha_{A'} = \dfrac{1}{1 - \lambda_2} = \dfrac{1}{1 - \frac{1}{\lambda_1'}} = \dfrac{\lambda_1'}{\lambda_1' - 1}$.
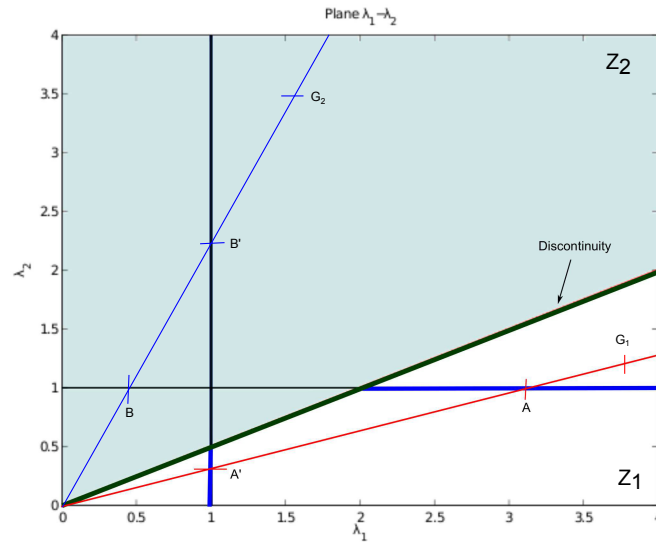

Figure 9. Plane $\lambda_1 - \lambda_2$. The firing rate vector when λ_2 is varied (i.e., $\boldsymbol{\lambda} = [1\ \lambda_2]^T$) is composed of the points in line A′B′; its corresponding equilibrium throughput is shown in Figure 8b. Multiplying such a vector by $k = \frac{1}{\lambda_2}$ results in $\boldsymbol{\lambda'} = [\frac{1}{\lambda_2}\ 1]^T$, a vector described by the points in line BA; its equilibrium throughput is depicted in Figure 8c.

The other two intervals can be determined in the same way. For $\lambda_2 = 0.5$ it is obvious, and for $0.5 < \lambda_2$, points B and B' are used. The equilibrium throughput of the system under variation of λ_1', $\boldsymbol{f'}_e = \alpha'\boldsymbol{x}$, is represented in Table 4.

Table 4. Equilibrium throughput w.r.t. λ_1 and its characteristics of the MTS net depicted in Figure 8a.

	Equilibrium Throughput w.r.t. λ_1		
λ_1' **Interval**	**Equilibrium Throughput** $\boldsymbol{f'}_e$	m_e **Activates Configuration:**	m_e **Belongs to Region:**
$0 < \lambda_1' < 2$	$\alpha' = \dfrac{10\lambda_1'}{2 + \lambda_1'}$	$\mathcal{C}_{13} = (p_1, t_1), (p_3, t_2)$	$\mathcal{R}_{13}$
$\lambda_1' = 2$	$\alpha' = 5$	$\mathcal{C}_{11} = (p_1, t_1), (p_1, t_2)$ and $\mathcal{C}_{13} = (p_1, t_1), (p_3, t_2)$	$\mathcal{R}_{11} \cap \mathcal{R}_{13}$
$\lambda_1' > 2$	$\alpha' = \dfrac{\lambda_1'}{\lambda_1' - 1}$	$\mathcal{C}_{21} = (p_2, t_1), (p_1, t_2)$	$\mathcal{R}_{21}$

This is depicted in Figure 8c, and a *cached* non-monotonicity (or decreasing) of the equilibrium throughput is now observed (there is a jump from a higher value $\boldsymbol{f'}_e = 5x$ to a lower one $\boldsymbol{f'}_e = 2x$ in the discontinuity value).

Notice that the reasoning used in previous example can be generalized to any TCPN, when a discontinuity in its equilibrium throughput appears due to the variation of a firing rate λ_i: the system throughput is non-monotonic with respect to $\boldsymbol{\lambda}$. This is formalized in the following theorem (written in the contrapositive form).

Theorem 2 ([14]). *Let $\langle N, \boldsymbol{\lambda}, \boldsymbol{m}_0 \rangle$ be an MTS TCPN system with $\boldsymbol{m}_0$ fixed and $\boldsymbol{\lambda}$ arbitrary. If the equilibrium throughput is monotonic with respect to $\boldsymbol{\lambda}$, then it is continuous with respect to $\boldsymbol{\lambda}$.*

The upper part of the diagram of Figure 10 shows the relations among continuity, monotonicity, and deadlock-free monotonicity. The left side, implication (a), is Theorem 2. Focusing on the right side and taking into account Definition 6, a monotonic system never decreases its system throughput when the firing rates are increased, thus it cannot be zero. Hence, the system should be deadlock-free monotonic (arrow (b)), which is formalized in the next statement.
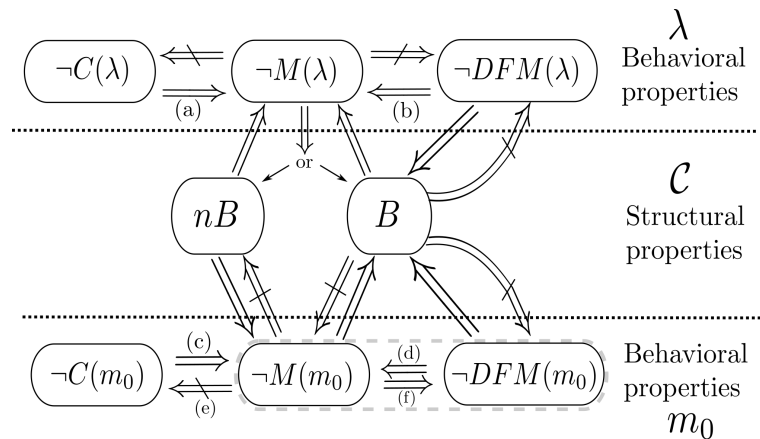

Figure 10. Relationships between configurations and behavioral properties. Continuity, monotonicity, and deadlock-free monotonicity w.r.t. the firing rates are abbreviated as $C(\lambda)$, $M(\lambda)$, and $DFM(\lambda)$, respectively. In the same way, continuity, monotonicity, and deadlock-free monotonicity w.r.t. the initial marking are abbreviated as $C(m_0)$, $M(m_0)$, and $DFM(m_0)$, respectively. Abbreviations nB and B stand for nB-Problematic systems and B-Problematic systems, respectively.

Proposition 4. *Let $\langle N, \lambda, m_0 \rangle$ be an MTS TCPN system with m_0 fixed and λ arbitrary. If the equilibrium throughput is monotonic with respect to λ, then it is deadlock-free monotonic with respect to λ.*

Proof. It derives directly from Definition 6. □

The reverse of implications (a) and (b) in Figure 10 are not true, an example of this can be found in Figure 2 of [15]. Moreover, another example is approached in Section 5.

4.2. A "Dual" Perspective: The Initial Marking Variation Case

In this case, formal definitions for discontinuities and non-monotonicities are given taking now the initial marking as a parameter. More precisely, these equilibrium throughput behaviors are defined when λ is fixed and m_0 varies.

Definition 7. *Let $\langle N, \lambda, m_0 \rangle$ be an MTS TCPN system with λ fixed. Assume that the initial marking m_0 is arbitrary. Its equilibrium throughput is:*

- Monotonic *with respect to the* initial marking, *denoted as $M(m_0)$, if $\forall(m_0, m_0')$, $m_0 \le m_0' \implies \alpha(m_0) \le \alpha(m_0')$;*
- Deadlock-free monotonic *with respect to the* initial marking, *denoted as $DFM(m_0)$, if $\forall(m_0, m_0')$ with $m_0 \le m_0'$, $\alpha(m_0) > 0 \implies \alpha(m_0') > 0$;*
- Continuous *with respect to the* initial marking, *denoted as $C(m_0)$, if for every m_0, given $\epsilon > 0$, there is $\delta > 0$ such that $\|m_0 - m_0'\|_2 < \delta \implies \|\alpha(m_0) - \alpha(m_0')\|_2 < \epsilon$, where $\|\cdot\|_2$ is the euclidean norm.*

A discontinuity of the equilibrium throughput due to smooth variations of the initial marking can occur, as can be seen in Figure 2a. A similar procedure to the previous one, for the analysis of this behavior with respect to the initial marking variations, can be carried out using the homothecy property to obtain the following result (arrow (c) in Figure 10).

Theorem 3 ([15]). *Let $\langle N, \lambda, m_0 \rangle$ be an MTS TCPN system with λ fixed and m_0 arbitrary. If the equilibrium throughput is monotonic with respect to m_0, then it is continuous with respect to m_0.*

Furthermore, directly derived from Definition 7, a monotonic system never decreases its system throughput when the initial markings are increased, thus its throughput cannot be zero. Hence, the system is also deadlock-free monotonic (arrow (d) in Figure 10).

Proposition 5. *Let $\langle N, \lambda, m_0 \rangle$ be an MTS TCPN system with λ fixed and m_0 arbitrary. If the equilibrium throughput is monotonic with respect to m_0, then it is deadlock-free monotonic with respect to m_0.*

Proof. It derives directly from Definition 7. □

The lower part of the diagram of Figure 10 shows these results, arrows (c) and (d). Our running example shows that, when initial marking variations are considered, a non-monotonic systems does not imply a discontinuous system, arrow (e). The implication represented by arrow (f) is discussed in Section 5. The relationships between these behaviors and the bifurcations of the equilibrium marking, give us an insight that the configurations of the net could provide some information about it. The structural properties that configurations provide are related to the behavioral properties observed in the equilibrium throughput of the TCPN system. Section 5 is devoted to clarify this fact.

5. Configurations, Continuity, and Monotonicity in MTS

Section 4 illustrated how discontinuities imply non-monotonicities in the equilibrium throughput. Now, we will see that undesired behaviors only occur when the equilibrium markings belong to regions of the reachable marking in which the associated T-covertures do not contain the support of a P-semiflow.

For instance, the discontinuity that appears in the equilibrium throughput of our running example (Figure 1a) occurs when the equilibrium marking belongs to configuration $\mathcal{C}_{1,2,10,11,8,6,7}$ (see Figure 4). Its associated net has no P-Semiflows, but there is a P-flow $y^T = [-1 \ -1 \ 0 \ 0 \ 0 \ 0 \ -1 \ 1 \ 0 \ 1 \ 1 \ 0]$. Moreover, the deadlocks shown in Figure 2, either with respect to the initial marking or with respect to the firing rates, have an equilibrium marking belonging to configuration $\mathcal{C}_{1,8,10,11,8,6,7}$ with associated subnet in Figure 5a; now, a subnet in which there are no P-Semiflows and no P-flows.

Section 3 showed that with varying λ_2 in the net depicted in Figure 1b, a discontinuity appears in the equilibrium throughput. This is possible because the subnet does not contain a P-flow; hence, no token conservation laws are present in the subnet even if the whole net is conservative. The fact that configurations without P-flows lead to a undesired equilibrium throughput can be generalized, as will be shown in Section 5. Now, configurations are classified into *suitable* or *problematic* to systematically study, from a structural point of view (parametrized by the equilibrium marking), the equilibrium throughput behavior in Mono-T-semiflow TCPN systems when the firing rates vary.

Definition 8. *A configuration $\mathcal{C}_i$, of an MTS net N, is said to be:*

1. Suitable *if the support of a P-semiflow is contained in its T-coverture:*

$$\exists y \gneq 0 \mid y^T C = 0 \text{ and } \|y\| \subseteq \mathcal{T}(\mathcal{C}_i).$$

   Otherwise, $\mathcal{C}_i$ is termed a problematic *configuration.*
2. nB-Problematic *if its T-coverture does not contain the support of a P-semiflow and it contains the support of a P-flow.*
3. B-Problematic *if its T-coverture does not contain the support of P-semiflows nor P-flows.*

B- and nB- refer to the existence or nonexistence of *bifurcations* (jumps) in the equilibrium throughput, respectively, as already discussed in Section 3.

Given a configuration of a net, deciding if it is suitable is quite simple. It can be checked using a linear algebraic problem: find if there exists a P-semiflow $\boldsymbol{y}$, whose support belongs to the T-coverture of the configuration, $\|\boldsymbol{y}\| \in \mathcal{T}_{\mathcal{C}}$. If the configuration is not suitable, then it remains to be decided if it is B-Problematic or nB-Problematic. This can also be checked with a linear algebraic problem: find if there exists a P-flow $\boldsymbol{y}$, whose support belongs to the T-coverture of the configuration, $\|\boldsymbol{y}\| \in \mathcal{T}_{\mathcal{C}}$. If it exists, the configuration is nB-Problematic. This is equivalent to check the rank of the token-flow matrix, if $rank(\boldsymbol{C}_{\mathcal{T}_{\mathcal{C}}}) < |\mathcal{T}_{\mathcal{C}}|$, then the configuration is nB-Problematic; otherwise, it is B-Problematic. Algorithm 3 performs this verification and runs in polynomial time.

In Figure 4, the first two configurations $\mathcal{C}_{1,2,3,4,5,6,7}$ and $\mathcal{C}_{1,8,3,4,8,6,7}$ are suitable since they have a P-semiflow, $\boldsymbol{y}^T = [1\ 1\ 1\ 1\ 1\ 1\ 1\ 0\ 0\ 0\ 0\ 0]$ and $\boldsymbol{y}^T = [0\ 0\ 1\ 0\ 0\ 1\ 0\ 1\ 0\ 0\ 0\ 0]$, respectively. Configuration $\mathcal{C}_{1,2,10,11,8,6,7}$ is nB-Problematic since it does not have any P-semiflow, but it has the P-flow $\boldsymbol{y}^T = [-1\ -1\ 0\ 0\ 0\ 0\ -1\ 1\ 0\ 1\ 1\ 0]$. Configuration $\mathcal{C}_{9,8,10,11,8,6,7}$ is B-Problematic since it has no P-flows (and thus, no P-semiflows).

Definition 9. *Let $\langle N, \boldsymbol{\lambda}, \boldsymbol{m}_0 \rangle$ be an MTS TCPN system.*

- *The system is* suitable, *denoted by $\boldsymbol{S}$, if every reachable equilibrium marking $\boldsymbol{m}_e$ activates a suitable configuration,*
- *The system is* nB-Problematic, *denoted by $\boldsymbol{nB}$, if every reachable equilibrium marking $\boldsymbol{m}_e$ that does not activate a suitable configuration, activates only nB-Problematic configurations.*
- *The system is* B-Problematic, *denoted as $\boldsymbol{B}$, if there exists a reachable equilibrium marking $\boldsymbol{m}_e$ that does not activate a suitable configuration, but activates a B-Problematic one.*

Algorithm 3 Computing the type of a given configuration.

Require: N and configuration $\mathcal{C}$.
Ensure: The type of configuration
1: Compute the T-coverture of $\mathcal{C}$: $\mathcal{T}_{\mathcal{C}}$.
2: Compute the token-flow matrix of the associated subnet: $\boldsymbol{C}_{\mathcal{T}_{\mathcal{C}}}$.
3: $\mathcal{P}_3 : \left\{ \text{Find } \boldsymbol{y} \geq \boldsymbol{0} \text{ s.t. } \boldsymbol{y}^T \boldsymbol{C}_{\mathcal{T}_{\mathcal{C}}} = 0 \wedge \sum_{p_i \in \mathcal{T}_{\mathcal{C}}} \boldsymbol{y}(p_i) \geq 1 \wedge \forall p_j \notin \mathcal{T}_{\mathcal{C}}, \boldsymbol{y}(p_j) = 0 \right\}$
4: **if** $\mathcal{P}_3$ has a solution **then**
5:    $\mathcal{C}$ is suitable
6: **else**
7:    **if** $rank(\boldsymbol{C}_{\mathcal{T}_{\mathcal{C}}}) = |\mathcal{T}_{\mathcal{C}}|$ **then**
8:       $\mathcal{C}$ is B-problematic
9:    **else**
10:       $\mathcal{C}$ is nB-problematic
11:    **end if**
12: **end if**

Figure 10 shows a complete picture of the relationships that exist between the reachable configurations of a system and the equilibrium properties of the equilibrium marking (monotonicity, continuity, and deadlock-free monotonicity), with respect to the initial marking and the firing rates. The upper and lower part of that diagram were discussed in Section 4.

Discontinuities of the equilibrium throughput, either with respect to the firing rates or with respect to the initial markings, imply the non-monotonicity of the system. In the case of the firing rate variation, the non-monotonicity implies that the equilibrium marking is reaching regions in which the associated configuration is problematic. Moreover, the converse is also true.

Theorem 4 ([14]). *Let $(N, \boldsymbol{\lambda}, \boldsymbol{m}_0)$ be an MTS TCPN system. The following two statements are equivalent:*

1. *Every reachable equilibrium marking activates a suitable configuration.*
2. *The equilibrium throughput is monotonic with respect to λ.*

For example, continuing with the manufacturing system depicted in Figure 1. Let the initial marking be fixed to $m_0 = \begin{bmatrix} 13\ 0\ 0\ 0\ 0\ 0\ 0\ 5\ 7\ 4\ 4\ 7 \end{bmatrix}^T$, and the firing rates $\lambda = \begin{bmatrix} 1\ 1\ 1\ 1\ \lambda_5\ 1\ 1 \end{bmatrix}^T$. Increasing the firing rate λ_5, the equilibrium throughput exhibits a discontinuity as can be seen in Figure 11a. Since this system is discontinuous, according to the relations shown in Figure 10, it is also non-monotonic. This behavior occurs particularly when the firing rate λ_2 is increased, as is illustrated by Figure 11b. In this last case, the system reaches a deadlock for any λ_2 greater than λ_5.

Now, if the initial marking is set to $m_0 = \begin{bmatrix} 13\ 0\ 0\ 0\ 0\ 0\ 0\ 6\ 7\ 4\ 4\ 7 \end{bmatrix}^T$, one more mark in place p_8, then the system cannot reach a deadlock for any value of the firing rates. This can be explained thanks to the P-flow $y^T = [-1\ -1\ 0\ 0\ 0\ 0\ -1\ 1\ 0\ 1\ 1\ 0]$. The invariant law $y^T m_0 = y^T m$ gives that $1 = m(p_8) + m(p_{10}) + m(p_{11}) - m(p_1) - m(p_2) - m(p_7)$, and mathematically implies that the deadlock marking (where all those places must be zero) cannot be reached. The physical meaning is that the number of resources, $m_0(p_8) = 6$, together with the capacity of the processing machine ($m_0(p_{10}) = 4$ and $m_0(p_{11}) = 4$), are greater than the number of products that the system handles, $m_0(p_1) = 13$. This prevents the blocking situation. Nonetheless, the system is non-monotonic, as can be seen in Figure 11c.
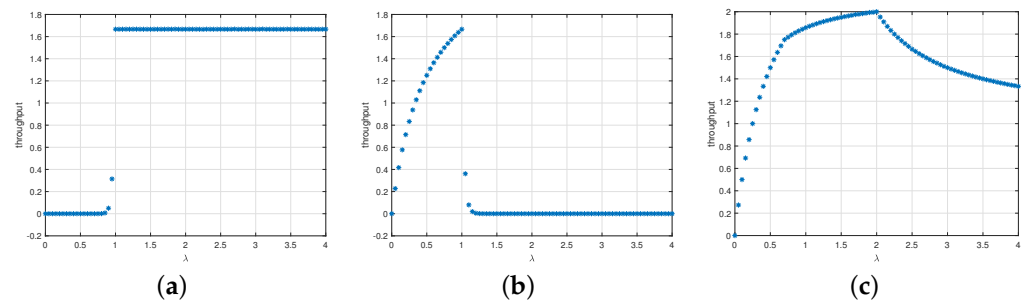

Figure 11. Equilibrium throughput properties of the MTS TCPN model in Figure 1b. (**a**) Discontinuity of the equilibrium throughput for parameter λ_5. (**b**) Non-monotonicity with deadlock of the equilibrium throughput for parameter λ_2. (**c**) Non-monotonicity without deadlock of the equilibrium throughput for parameter λ_2.

In these cases, the equilibrium marking reaches regions in which the associated configuration is not suitable. In Figure 11a,b, a region with B-Problematic configuration $\mathcal{C}_{1,8,10,11,8,6,7}$ is reached and that is why the discontinuity induced bifurcation and the deadlocks appear (the configuration reached is associated with the subnet in Figure 5a). This is formalized in the next theorem.

Theorem 5 ([15]). *Let $\langle N, \lambda, m_0 \rangle$ be an MTS TCPN system with λ fixed and m_0 arbitrary. If the equilibrium throughput is not deadlock-free monotonic with respect to m_0, then there exists an equilibrium marking m_e that activates only a B-Problematic configuration.*

For the case of Figure 11c, a region with nB-Problematic configuration $\mathcal{C}_{1,2,10,11,8,6,7}$ is reached and that is why the system presents a decrement of the equilibrium throughput. It is the same subnet of Figure 5a with the additional place p_2; this place induces a restriction that prevents the system of reaching the deadlock. This is formalized in the next proposition.

Proposition 6 ([15]). *Let $\langle N, \lambda, m_0 \rangle$ be an MTS TCPN system with λ fixed and m_0 arbitrary. If every reachable equilibrium marking m_e, which does not activate a suitable configuration, activates only an nB-Problematic configuration, then the equilibrium throughput is non-monotonic with respect to m_0.*

Now, let us set the firing rate to $\lambda = \begin{bmatrix} 1\,3\,1\,1\,1\,1\,1 \end{bmatrix}^T$, and the initial marking to $m_0 = \begin{bmatrix} k_1\,0\,0\,0\,0\,0\,6\,7\,4\,4\,7 \end{bmatrix}^T$, where k_1 is taken as a variation parameter. If this initial marking is increased, then the equilibrium throughput exhibits a non-monotonic behavior, as can be seen in Figure 12. This complements the above explanation that the number of resources, together with the capacity of the machine, should be greater than the products that the system can handle, so that no blocking situations occur.
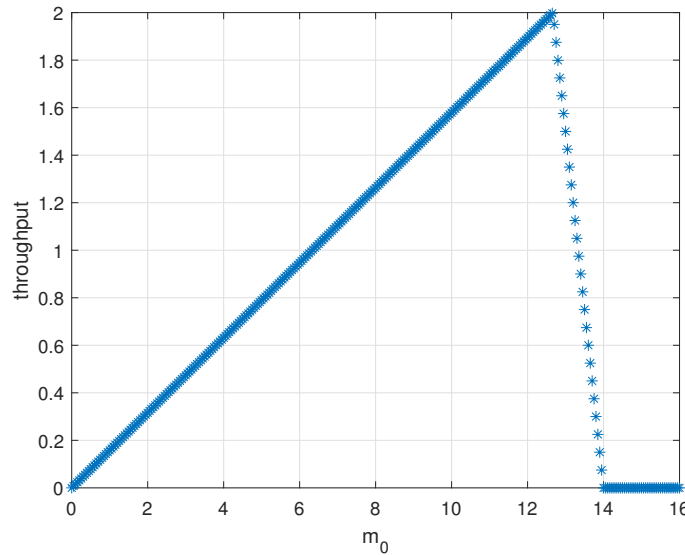
Figure 12. Non-monotonicity of the system in Figure 1b with the deadlock of the equilibrium throughput for parameter $m_0(p_1) = k_1$.

In this case, the equilibrium marking reaches the region with nB-Problematic configuration $\mathcal{C}_{1,2,10,11,8,6,7}$ (decreasing part of the equilibrium marking), and finally reaches a region associated with the B-Problematic configuration $\mathcal{C}_{1,8,10,11,8,6,7}$.

As can be seen in Theorems 4 and 5 and Proposition 6, the study of the equilibrium throughput properties depends not only on the type of the configuration (suitable or problematic), but also on the possibility that this configuration becomes activated from the initial marking. As mentioned above, Algorithm 3 decides the type of a configuration; now, Algorithm 4 determines when the configuration can be activated.

Algorithm 4 Computing if a given configuration can be activated by an equilibrium marking.

Require: $\langle N, \lambda, m_0 \rangle$, configuration $\mathcal{C}$.
Ensure: If configuration $\mathcal{C}$ may be activated by an equilibrium marking
  1: Compute the token-flow matrix $\boldsymbol{C} = \boldsymbol{Post} - \boldsymbol{Pre}$
  2: Compute a basis of P-semiflows $\boldsymbol{B}_y$
  3: Compute the existence of a reachable equilibrium marking activating $\mathcal{C}$:
     $\mathcal{P}_4$: { Find $m \geq 0$ such that
       1. $\boldsymbol{B}_y^T m = \boldsymbol{B}_y^T m_0$; {Reachable marking}
       2. $\boldsymbol{C \Lambda \Pi}_{\mathcal{C}} m = \boldsymbol{0}$; {Equilibrium marking}
       3. $\forall (p_i, t_j) \in \mathcal{C}, \frac{m(p_i)}{\boldsymbol{Pre}(p_i,t_j)} \leq \frac{m(p_k)}{\boldsymbol{Pre}(p_k,t_j)}$ }; {marking activates configuration $\mathcal{C}$}
  4: **if** $\mathcal{P}_4$ has a solution **then**
  5:    $\mathcal{C}$ may be activated
  6: **else**
  7:    $\mathcal{C}$ cannot be activated
  8: **end if**

In order to know if a given configuration can be activated, the Algorithm 4 performs a search of a marking m that satisfies the following restrictions: m is a positive reachable

marking, m is an equilibrium marking, for every arc of the configuration, the place that restricts the transition flow belongs to the T-coverture. It represents a unique system of linear inequalities that can be solved in polynomial time.

For the TCPN system in Figure 8a, Algorithm 4 can decide if the problematic configuration $\mathcal{C}_{11} = \{(p_1, t_1), (p_1, t_2)\}$ can be activated with $m \geq 0$. The system of inequalities is:

$$\begin{bmatrix} 1 & 0 & 1 \\ 0 & 1 & 1 \end{bmatrix} m = \begin{bmatrix} 10 \\ 9 \end{bmatrix}, \quad \mathcal{P}_4 - 1$$
$$C\Lambda\Pi_{\mathcal{C}}m = 0, \quad \mathcal{P}_4 - 2$$
$$\frac{m(p_1)}{2} \leq \frac{m(p_2)}{1}, \quad \mathcal{P}_4 - 3$$
$$\frac{m(p_1)}{1} \leq \frac{m(p_3)}{1}, \quad \mathcal{P}_4 - 3$$

For this case, Algorithm 4 finds that the configuration $\mathcal{C}_{11}$ can be activated, because the equilibrium marking $m = [5\,4\,5]^T$ is a solution of problem $\mathcal{P}_4$.

Related with Theorem 4, if there exists a marking that can reach a problematic configuration, then the system will be non-monotonic. The system also has the possibility to be non deadlock-free monotonic, as happens when the initial marking is $m_0 = [13\,0\,0\,0\,0\,0\,0\,5\,7\,4\,4\,7]^T$ in the manufacturing system. Algorithm 5 determines if the system can reach a deadlock regardless of the firing rate. It searches for a marking fulfilling the following restrictions: m is a positive reachable marking and every place of the corresponding T-coverture has a zero marking. Again, Algorithm 5 solves a unique system of linear inequalities, and it runs in polynomial time. If for every reachable configuration there are no blocking markings, then the system is deadlock-free monotonic.

Algorithm 5 Computing if there exists a deadlock marking in a given configuration.

Require: $\langle N, m_0 \rangle$, a problematic configuration $\mathcal{C}$, matrix configuration $\Pi_{\mathcal{C}}$.
Ensure: If there exists a blocking marking
 1: Compute the token-flow matrix $C = Post - Pre$
 2: Compute a basis of P-semiflows B_y
 3: Compute the existence of a reachable deadlock marking activating $\mathcal{C}$:
    $\mathcal{P}_5$: { Find $m \geq 0$ such that
    1. $B_y^T m = B_y^T m_0$
    2. $\forall (p_i, t_j) \in \mathcal{C}, m(p_i) = 0$ }
 4: **if** $\mathcal{P}_5$ has a solution **then**
 5:   m is a blocking marking
 6: **else**
 7:   There are not blocking markings
 8: **end if**

From Theorem 5 and Proposition 6, it is possible to derive the following structural result. Referring to Figure 10, Proposition 6 represents the arrow going from nB to $\neg M(m_0)$, and Theorem 5 represents the arrow going from $\neg M(m_0)$ to B. The meaning of this relation is that if there exists an nB-Problematic configuration in N, then there exists also a B-Problematic configuration.

Proposition 7 ([15]). *Let N be an MTS net. If there exists an nB-Problematic configuration, then there exists a B-Problematic configuration.*

Finally, because of this implication, it is possible to conclude that: *a non-monotonic system, with respect to initial marking variations, is also non deadlock-free monotonic.*

Theorem 6 ([15]). *Let* $\langle N, \lambda, m_0 \rangle$ *be an MTS TCPN system with* λ *fixed and* m_0 *arbitrary. The equilibrium throughput is a deadlock-free monotonic with respect to* m_0 *iff it is monotonic with respect to* m_0.

Reviewing the flow equation $f = \Lambda \Pi_{\mathcal{C}} m$, it could be concluded that both the firing rate Λ and marking m affects in an analogous way to the system flow (a kind of duality), since f depends directly on both factors. Nevertheless, when Figure 10 is analyzed in detail, some differences on how the undesired throughput behaviors are related with each other, with initial marking and firing rate variations, appears. This is why it can be seen as a *weak duality*.

This happens because, although both are analogously affecting the system flow, once again, the marking evolves with the time while the firing rates remain constant. To clarify this, consider the state equation of the system $\dot{m} = C\Lambda \Pi_{\mathcal{C}} m$. Obviously, the matrix Λ is affecting the dynamic matrix of the mode $A_{\mathcal{C}} = C\Lambda \Pi_{\mathcal{C}}$, i.e., affecting the eigenvalues of the dynamic matrix. The initial marking m_0 gives the initial condition of the state equation and the marking is evolving according to this equation. Hence, these values play different roles in the system evolution.

6. Reduction Rules

According to what has been previously established, when looking for undesired behaviors in an MTS TCPN system, it is important to see if there exist problematic configurations that can be activated. A first step may be to verify if there are problematic configurations in the net. If there are no problematic configurations, then the considered undesired behaviors cannot appear in the system. Otherwise, the initial marking has to be considered to analyze if the problematic configurations can be activated.

As already mentioned, the number of configurations of a net may be exponential with the net size. Thus, searching for problematic configurations can be computationally expensive. Even if the Algorithm 3 runs in polynomial time, the number of configurations in a net can make the evaluation of every configuration impractical. In this sense, the CPN system may be polynomially pre-processed before the computation of problematic configurations, so that the total number of configurations to be analyzed is reduced. The purpose of this pre-processing is to reduce the computational problem, but the theoretical problem still remains. Nonetheless, it results very useful for many practical systems that can be found in manufacturing systems, chemical reactions, and healthcare systems, among others. Now, a set of reduction rules (see [16] for a more general and technical presentation) are intuitively explained for very particular cases in order to present an analysis on how to reduce systems maintaining its configuration properties.

As mentioned before, our running example of Figure 1b has 64 configurations. It is possible to evaluate all these configurations using Algorithm 3 in order to determine if there exist problematic configurations and their type (B- or nB-Problematic). After 64 steps, the algorithm finds (see Figure 4) that:

1. Two of these configurations are B-Problematic, with associated T-covertures:

$$\mathcal{T}_{\mathcal{C}_{1,8,10,11,8,6,7}} = \{p_1, p_6, p_7, p_8, p_{10}, p_{11}\},$$

$$\mathcal{T}_{\mathcal{C}_{9,8,10,11,8,6,7}} = \{p_6, p_7, p_8, p_9, p_{10}, p_{11}\}$$

2. One of them is nB-Problematic, with associated T-coverture:

$$\mathcal{T}_{\mathcal{C}_{1,2,10,11,8,6,7}} = \{p_1, p_2, p_6, p_7, p_8, p_{10}, p_{11}\}$$

3. The other 61 configurations are suitable.

Figure 13 shows a reduction process of our running example, which is explained below. The intention of this reductions is to maintain the problematic configurations or the

ability to recover them from the reduced net. More importantly, the reductions allow to gain insights about the structures that produce problematic configurations, which cause the undesired behaviors of the equilibrium throughput.
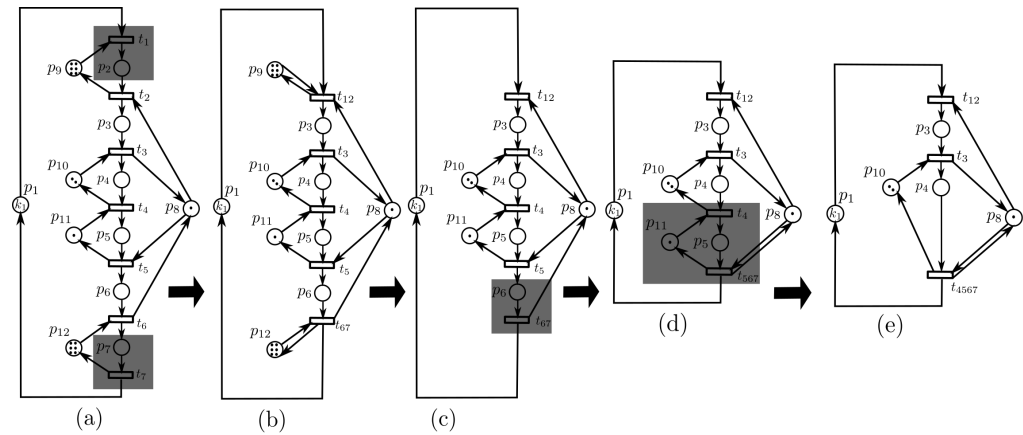

Figure 13. Reduction process of a net model. (**a**) Original net model, post-fusion of transitions t_6 and t_7, and pre-fusion of t_1 and t_2 are shaded. (**b**) First reduced net with self-loop places that can be removed. (**c**) Second reduced net, post-fusion of transitions t_5 and t_{67} is shaded. (**d**) Third reduced net, macrotransition is shaded. (**e**) Final reduced net.

Let us focus first on transition t_7. One can notice that it has one input place (it is said to be *essential* in the coverture). Hence, every configuration of the net must contain the arc (p_7, t_7); thus, every T-coverture of the net contains place p_7. From this fact, it is evident that a problematic configuration cannot contain the arc (p_{12}, t_6), because place p_{12} would be contained in its T-coverture, and p_7 and p_{12} are the support of a P-semiflow. This can be captured using two reduction rules:

1. A *post-fusion* of transitions can be performed for transitions t_6 and t_7. Their structure is a particular case of the third reduction rule in Figure 14. It keeps the same number of configurations in the reduced net, and it is possible to establish that every problematic configuration of the reduced net has its corresponding problematic configuration in the original one. A detailed explanation of this fact is exposed in Proposition 4 in [16].
2. The reduction of transitions t_6 and t_7 makes (in the neighboring of this part of the reduced net) that p_{12} becomes a marked self-loop place. This place can be removed following the idea of the *implicit* place for continuous Petri nets discussed in [19]. This particular structure is a marked P-semiflow of the net, even when it restricts the behavior of the system, its elimination allows to remove several configurations. In this particular case, after the transformation, the reduced net has now 32 configurations in contrast with the 64 configurations of the original one.

Now, paying attention to transition t_1, one can notice that its input places are p_1 and p_9. This transition is the only input of place p_2, which in turn, only have the output transition t_2. Roughly speaking, the enabling of t_2 depends indirectly on the marking of places p_1 and p_9. A *pre-fusion* of transitions t_1 and t_2 can be performed in the net, obtaining a reduced net in which the T-covertures of the problematic configurations are related to the ones of the original net, except that the "absorved" place p_2 is not present in the T-covertures of the reduced net. This reduction is a particular case of the forth rule depicted in Figure 14, which is explained in detail in Proposition 5 of [16].

As in the previous reduction, a *self-loop* place p_9 is obtained after the pre-fusion of those transitions. Once again, this place is structurally implicit (particularly, an isolated and marked P-semiflow) and can be removed. Therefore, a reduced net in which there are 16 configurations is obtained. Again, a post-fusion between transitions t_5 and t_{67} can be performed obtaining a reduced net in which the number of configurations remains (16 configurations).

Transitions t_4 and t_{567} together with places p_5 and p_{11} form a strongly connected choice-free net, which is also consistent (in particular, it is a simple circuit). Obviously, the P-semiflows inside this subnet should be initially marked, otherwise the system would be blocked. The reduction of this local structure is identified as a *macrotransition* according to Definition 14 in [16]. It is shown as the second rule in Figure 14. This reduction can be performed in a net maintaining its problematic configurations, because no choice places are removed in it.
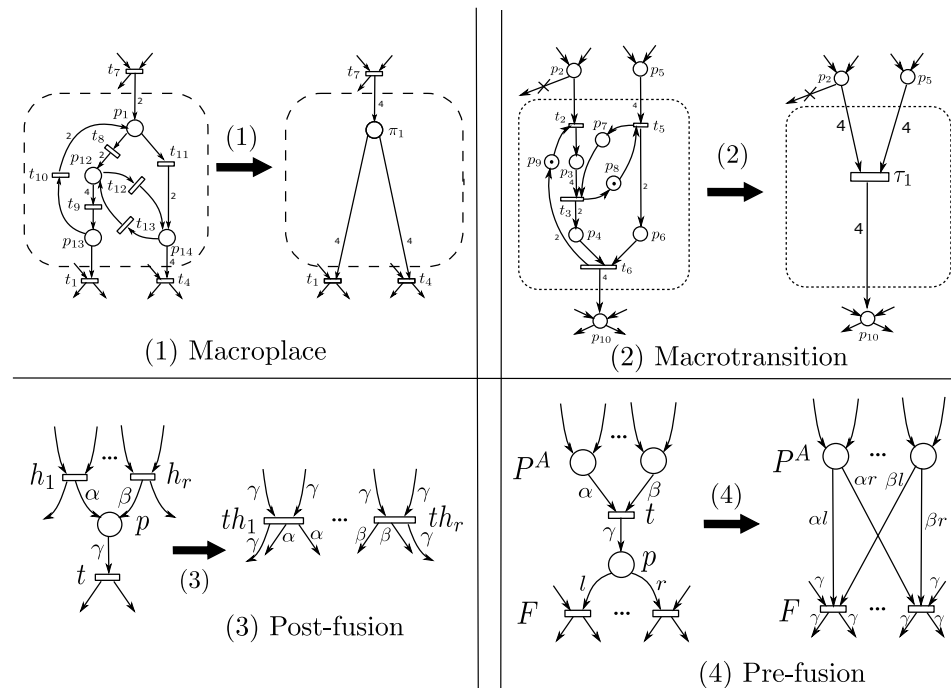

(1) Macroplace

(2) Macrotransition

(3) Post-fusion

(4) Pre-fusion

Figure 14. Particular examples of reduction rules preserving problematic configurations from [16].

The dual concept of the macrotransition is the *macroplace* (see the first rule in Figure 14). In this case, the places and transitions in the identified subnet form a strongly connected join-free net, which is also conservative. The configurations of the reduced net are mostly the same as the original, because no join transitions are removed during the procedure. A detailed discussion about this rule can be found in [16].

Finally, for the reduced net in Figure 13e with eight configurations, Algorithm 3 can be applied to decide if these configurations are problematic. This reduced net has one B-Problematic configuration, whose associated T-coverture is $\mathcal{T}_{\mathcal{C}_{8,10,8}} = \{p_8, p_{10}\}$, and one nB-Problematic configuration, whose T-coverture is $\mathcal{T}_{\mathcal{C}_{1,10,8}} = \{p_1, p_8, p_{10}\}$.

Now, if we want to obtain the problematic configurations of the original net from the reduced one, this can be done going backwards in the transformation path carried out.

- From the net in Figure 13e, configuration $\mathcal{C}_{8,10,8}$ is B-Problematic. Its T-coverure is $\mathcal{T}_{\mathcal{C}_{8,10,8}} = \{p_8, p_{10}\}$, where we can see that places p_1, p_3, and p_4 are not part of the problematic configuration in the reduced net, and thus, they are not in the original one.
- From the net in Figure 13d, if p_4 and p_3 are not used, then necessarily, p_{11} and p_{10} should be in the original problematic T-coverture. Thus, the recovered T-coverture at this point is $\mathcal{T}_{\mathcal{C}_{8,10,11,8}} = \{p_8, p_{10}, p_{11}\}$.
- From the net in Figure 13c, we can see that place p_6 is an essential cover of the net; thus, it should be in the original T-coverture. Hence, the recovered T-coverture at this point is $\mathcal{T}_{\mathcal{C}_{8,10,11,8,6}} = \{p_6, p_8, p_{10}, p_{11}\}$.
- From the net in Figure 13b, places p_9 and p_{12} cannot be part of the problematic configuration, they represent P-semiflows in this net. Hence, the T-coverture at this point is $\mathcal{T}_{\mathcal{C}_{8,10,11,8,6}} = \{p_6, p_8, p_{10}, p_{11}\}$.

- From the net in Figure 13a, place p_7 is an essential cover, so it must be in the configuration. The previously removed place p_9 was involved in a pre-fusion of transitions, which in this net means that place p_2 ("absorved" in the pre-fusion) cannot be used. In this net, either place p_1 or p_9 can restrict the flow of transition t_1. Hence, we have two B-Problematic configurations, $\mathcal{C}_{1,8,10,11,8,6,7}$ and $\mathcal{C}_{9,8,10,11,8,6,7}$.

These last configurations are the two B-Problematic configurations that the original net has. A similar procedure can be carried out to obtain the nB-Problematic configuration of the original net from the reduced one.

These reductions provide an important insight about the roots of undesired behaviors. In particular, these reductions maintain the problematic configurations of those having choice places interacting inadequately with join transitions. In our running example, one B-Problematic configuration of the reduced net "captures" two B-Problematic configurations of the original net. This is because both configurations have the same problem in common, namely, the interaction between p_8 and t_3 is not adequate. A further discussion of this fact is also presented in [16].

7. Concluding Remarks

Equilibrium throughput is a performance index of manufacturing systems that measures in "steady state" the quantity of goods fabricated per unit time. When the manufacturing system is modeled as a TCPN, then the equilibrium throughput represents the transition flow. This flow depends on the net structure, the firing rate of transitions, and the TCPN initial marking. Given a net structure, from an engineering point of view, both the firing rate and the marking can be varied to modify the equilibrium throughput. However, despite the simple formula of the equilibrium throughput $f_e = \Lambda \Pi_{\mathcal{C}} m_e$, this work illustrated that a careful analysis must be carried out when those parameters vary. In fact, they may lead to very complex behaviors of the TCPN equilibrium throughput.

In particular, this work showed that the structural objects named problematic configurations are responsible that varying the initial marking or firing rate of transitions the equilibrium throughput of the net exhibits paradoxical behaviors, such as non-monotonicities and discontinuities. To explain those behaviors, we start by delineating how the equilibrium marking varies when the firing rate of transitions changes. In this case, the state equation $\dot{m} = C\Lambda \Pi_{\mathcal{C}} m$, $m \in \mathcal{R}_{\mathcal{C}}$, $\mathcal{C} \in S\mathcal{C}(N)$, $m(0) = m_0$ is used. This work points out that when there exist closed paths gaining/losing tokens and the firing rate of the transitions varies, the equilibrium marking may exhibit jumps, generating undesired behaviors, such as discontinuities and non-monotonicities, in the equilibrium throughput with respect to the variation of firing rates.

The structural objects named *problematic* configurations are considered to formally explain how the structure of the net determines the undesired behaviors in the equilibrium throughput. Those configurations highlight how the net structure participates in the generation of discontinuities and non-monotonicities in the equilibrium throughput when they vary the initial marking, m_0, or firing rates of transitions, λ.

Herein, we show that when the equilibrium marking exhibits a discontinuity w.r.t. firing rate variations, then it is non-monotonic w.r.t. firing rate variations, i.e., increasing the speed of the resources reduced the equilibrium throughput, which is an undesired effect. Moreover, if the equilibrium is not deadlock free w.r.t. firing rate variations, then it is non-monotonic w.r.t. firing rate variations. Similar properties are found when the initial marking varies instead of the firing rate.

It is worth to note that the number of configurations may grow exponentially in the number of join transitions. Nevertheless, a procedure to reduce the net, preserving the undesired equilibrium throughput behaviors, is described. It allows to face the problem of finding out a problematic configuration in a reasonable amount of computational time.

Conflicts of Interest: The authors declare no conflict of interest.

Abbreviations

The following abbreviations are used in this manuscript:

PN	Petri net
CPN	Continuous Petri net
TCPN	Timed continuous Petri net
DES	Discrete event system
FMS	Flexible manufacturing system
ISS	Infinite server semantics
FSS	Finite server semantics
PS	Product semantics
MTS	Mono-T-Semiflow
MTSR	Mono-T-Semiflow Reducible
CNC	Computer numerical control
CF	Choice-Free
JF	Join-Free
Ct	Consistent
Cv	Conservative
$C(\lambda)$	Continuous with respect to the firing rate
$M(\lambda)$	Monotonic with respect to the firing rate
$DFM(\lambda)$	Deadlock-Free Monotonic with respect to the firing rate
$C(m_0)$	Continuous with respect to the initial marking
$M(m_0)$	Monotonic with respect to the initial marking
$DFM(m_0)$	Deadlock-Free Monotonic with respect to the initial marking
nB	nB-Problematic system
B	B-Problematic system

References

1. David, R.; Alla, H. *Discrete, Continuous, and Hybrid Petri Nets*, 2nd ed.; Springer: Berlin, Germany, 2010.
2. Silva, M.; Teruel, E.; Colom, J.M. Linear algebraic and linear programming techniques for the analysis of place/transition net systems. In *Lectures on Petri Nets I: Basic Models: Advances in Petri Nets*; Reisig, W., Rozenberg, G., Eds.; Springer: Berlin/Heidelberg, Germany, 1998; pp. 309–373.
3. Fraca, E.; Haddad, S. Complexity Analysis of Continuous Petri Nets. *Fundam. Inform.* **2015**, *137*, 1–28. [CrossRef]
4. Mahulea, C.; Recalde, L.; Silva, M. Basic Server Semantics and Performance Monotonicity of Continuous Petri Nets. *Discret. Event Dyn. Syst.* **2009**, *19*, 189–212. [CrossRef]
5. Gudiño-Mendoza, B.; López-Mellado, E.; Alla, H. Modeling and simulation of water distribution systems using timed hybrid Petri nets. *Simulation* **2012**, *88*, 329–347. [CrossRef]
6. Silva, M.; Júlvez, J.; Mahulea, C.; Vázquez, C.R. On fluidization of discrete event models: Observation and control of continuous Petri nets. *Discret. Event Dyn. Syst.* **2011**, *21*, 427–497. [CrossRef]
7. Silva, M. Individuals, populations and fluid approximations: A Petri net based perspective. *Nonlinear Anal. Hybrid Syst.* **2016**, *22*, 72–97. [CrossRef]
8. Zimmermann, A. *Stochastic Discrete Event Systems. Modeling, Evaluation, Applications*; Springer: Berlin, Germany, 2007.
9. Silva, M.; Fraca, E.; Wang, L. Performance evaluation and control of manufacturing systems: A continuous Petri nets view. In *Formal Methods in Manufacturing*; Campos, J., Seatzu, C., Xie, X., Eds.; CRC Press: Boca Raton, FL, USA; Taylor & Francis: Abingdon, UK, 2014; pp. 409–452.
10. Júlvez, J.; Recalde, L.; Silva, M. Steady-state performance evaluation of continuous Mono-T-Semiflow Petri nets. *Automatica* **2005**, *41*, 605–616. [CrossRef]
11. Angeli, D.; Leenheer, P.D.; Sontag, E.D. A Petri net approach to the study of persistence in chemical reaction networks. *Math. Biosci.* **2007**, *210*, 598–618. [CrossRef] [PubMed]
12. Meyer, A. Discontinuity induced bifurcations in timed continuous Petri nets. In Proceedings of the 11th International Workshop on Discrete Event Systems (WODES), Guadalajara, Mexico, 3–5 October 2012; Volume 11, pp. 28–33.
13. Fraca, E.; Júlvez, J.; Silva, M. On the fluidization of Petri nets and marking homothecy. *Nonlinear Anal. Hybrid Syst.* **2014**, *12*, 3–19. [CrossRef]
14. Navarro-Gutiérrez, M.; Ramírez-Treviño, A.; Silva, M. Homothecy, bifurcations, continuity and monotonicity in timed continuous Petri nets under infinite server semantics. *Nonlinear Anal. Hybrid Syst.* **2017**, *26*, 48–67. [CrossRef]
15. Navarro-Gutiérrez, M.; Ramírez-Treviño, A.; Silva, M. Dual perspectives of equilibrium throughput properties of continuous mono-T-semiflow Petri nets: Firing rate and initial marking variations. *Automatica* **2022**, *136*, 110074. [CrossRef]

16. Navarro-Gutierrez, M.; Fraustro-Valdez, J.A.; Ramírez-Treviño, A.; Silva, M. Problematic configurations and choice-join pairs on Mono-T-Semiflow nets: Towards the characterization of behavior-structural properties. *Discret. Event Dyn. Syst.* **2020**, *30*, 175–209. [CrossRef]

17. Recalde, L.; Teruel, E.; Silva, M. Application and Theory of Petri Nets 1999. In Proceedings of the 20th International Conference, ICATPN'99, Williamsburg, VA, USA, 21–25 June 1999; Chapter Autonomous Continuous P/T Systems; Springer: Berlin/Heidelberg, Germany, 1999; pp. 107–126.

18. di Bernardo, M.; Budd, C.; Champneys, A.R.; Kowalczyk, P. *Piecewise-Smooth Dynamical Systems: Theory and Applications*; Springer Science & Business Media: Berlin/Heidelberg, Germany, 2008; Volume 163.

19. Recalde, L.; Mahulea, C.; Silva, M. Improving analysis and simulation of continuous Petri Nets. In Proceedings of the 2006 IEEE International Conference on Automation Science and Engineering, Shanghai, China, 8–10 October 2006; pp. 9–14.